Influence of solar forcing, climate variability and modes of low-frequency atmospheric circulation on summer floods in Switzerland

J.C. Peña[1], L. Schulte[2], A. Badoux[3], M. Barriendos[4] and A. Barrera-Escoda[1]

[1]{Meteorological Service of Catalonia, Barcelona, Spain}

[2]{Department of Physical and Regional Geography and ICREA, University of Barcelona, Barcelona, Spain}

[3]{Mountain Hydrology and Mass Movements Research unit, Swiss Federal Institute for Forest, Snow and Landscape Research WSL, Birmensdorf, Switzerland}

[4]{Catalan Institute of Climate Sciences (IC3) and Department of Modern History, University of Barcelona, Barcelona, Spain}

Correspondence to: L. Schulte (schulte@ub.edu)

Abstract

The higher frequency of severe flood events in Switzerland in recent decades has given fresh impetus to the study of flood patterns and their possible forcing mechanisms, particularly in mountain environments. This paper presents a new index of summer flood damage that considers severe and catastrophic summer floods in Switzerland between 1800 and 2009, and explores the influence of external forcings on flood frequencies. In addition, links between floods and low-frequency atmospheric circulation patterns are examined. The flood damage index provides evidence that the 1817-1851, 1881-1927, 1977-1990 and 2005-present flood clusters occur mostly in phase with palaeoclimate proxies. The cross-spectral analysis documents that the periodicities detected in the coherency and phase spectra of 11 (Schwabe cycle) and 104 years (Gleissberg cycle) are related to a high frequency of flooding and solar activity minima, whereas the 22-year cyclicity detected (Hale cycle) is associated with solar activity maxima and a decrease in flood frequency. The analysis of modes of low-frequency atmospheric variability shows that Switzerland lies close to the border of the summer principal mode: the Summer North Atlantic Oscillation. The Swiss river catchments situated

on the centre and southern flank of the Alps are affected by atmospherically unstable areas defined by the positive phase of the Summer North Atlantic Oscillation pattern, while those basins located in the northern slope of the Alps are predominantly associated with the negative phase of the pattern. Furthermore, a change in the low-frequency atmospheric circulation pattern related to the major floods occurred over the period from 1800 to 2009: the Summer North Atlantic Oscillation persists in negative phase during the last cool pulses of the Little Ice Age (1817-1851 and 1881-1927 flood clusters), whereas the positive phases of SNAO prevail during warmer climate of the last four decades (flood clusters from 1977 to present).

1 Introduction

The response of floods to global changes is complex and can vary on a regional scale. Extreme flood event frequency can be highly sensitive to modest environmental and climate changes (Knox, 2000), so much so, in fact, that these changes might not be recorded by mean hydrological values but rather by a changing pattern in the magnitude and frequency of extreme events (Benito et al., 2005). Moreover, these changes often occur during transitional stages of climatic pulses (Knox, 2000; Glaser and Stangl, 2004; Schulte et al., 2009a) and may respond to complex exogenic, endogenic and autogenic climate forcing mechanisms (Versteegh, 2005). Yet, the debate concerning the factors and trends that might influence flood dynamics, such as the rise in temperature, river management and other human activities, remains a controversial one (Brázdil et al., 2006).

In high mountain catchments, major flood events are determined by the intensity and frequency of extreme precipitation events, high discharge rates provoked by the melting of glacial ice and snow cover, the outburst flood of lakes dammed by landslides as well as by other phenomena. The Alps are highly sensitive to changes in atmospheric circulation and environmental perturbations that influence the hydrological regime and flooding patterns reconstructed from instrumental data and documentary sources (Hächler-Tanner, 1991; Röthlisberger, 1991; Gees, 1997; Pfister, 1999; Luterbacher et al., 2004; Weingartner and Reist, 2004; ALP-IMP, 2006; Burger, 2008; Schmocker-Fackel and Naef, 2010a, b; Wetter et al., 2011) and, regarding longer time series, from natural proxies such as lacustrine records, glaciers, dendrochronology and isotopic studies of speleothems (Tinner et al., 2003; Casty et al., 2005; Holzhauser et al., 2005; Boch and Spötl, 2008; Wilhelm et al., 2012). Referring to the last three millennia, the solar activity may be an important driver of alpine floods as indicated by the periodicities (Gleissberg solar cycles) of geochemical and pollen proxies of alluvial plain sediments in the Swiss Alps (Schulte et al., 2008, 2014) and by their correlation with climate proxies.

During the last 500 years, periods of large floods have been reported by detailed documentary inventories and instrumental series compiled by Röthlisberger (1991), Hächler-Tanner (1991), Gees (1997), Pfister (1999), Lehmann and Naef (2003), Vischer (2003), Burger (2008) and Hilker et al. (2009). According to the annual number of floods used by Schmocker-Fackel and Naef (2010a, b) as a parameter for the evaluation of the climate and hydric variability of catchments in Switzerland, increased flooding occurred during four main periods: 1560-1590, 1740-1790, 1820-1940 and 1970-2007. Since the second half of the 19th century, river correction and embankment may influence the frequency of flooding in the Swiss catchments. Other studies discuss the possible links between hydrological extreme events and low-frequency atmospheric circulation patterns (Pfister, 1999; Jacobeit et al., 2006; Knox, 2000; Glaser and Stangl, 2004; Mudelsee et al., 2004; Schmocker-Fackel and Naef, 2010b; Wilhelm et al., 2012), such as the North Atlantic Oscillation. However, in the Swiss Alps floods show a strong seasonal distribution recording highest frequencies during the summer months. Summer climate in the North Atlantic-European sector possesses a principal pattern of year-to-year variability similar to the North Atlantic Oscillation in winter, although this pattern is weaker and confined to northern latitudes. By analogy with the winter season, Folland et al., 2009 refer to this pattern of variability as the Summer North Atlantic Oscillation (SNAO). Our study of flood frequencies is focused on the influence of the SNAO which is defined as the main empirical orthogonal function of the standardized anomalies of the European mean sea level pressure (EMSLP) during July and August. The location of the action centres shows strong positive anomalies (high pressure centre) between the Scandinavia Peninsula and Great Britain, while the Mediterranean region is dominated by light negative anomalies (low pressure centre). The SNAO exerts a strong influence on rainfall, temperature and cloud cover through changes in the position of storm tracks in the North Atlantic region (Folland et al., 2009), but also in many areas of southern Europe (Bladé et al., 2011).

Our study aims to investigate the possible links between flood frequency in Switzerland and solar forcing, volcanic eruptions, climate variability and the North Atlantic dynamics over the last two centuries. A study of summer flood frequencies in Switzerland has been conducted for the period 1800-2009, based on the calculation of a flood damage index (henceforth INU) from existing flood inventories for Switzerland, summarizing both the severity of these events and their spatial extent. Special attention will be focused also on the possible different evolution between flood dynamics at the northern and southern slopes of the Alps during the last two centuries. The influence of solar and climate forcing on flood frequencies is investigated applying a cross-spectral analysis to the sunspot record and INU to determine the common periodicities, and we used temperature reconstruction, volcanic eruptions, Beryllium-10 records (solar activity) and oxygen isotope data (Greenland climate proxies) for finding links. Finally, the analysis of the possible links between floods and North Atlantic dynamics is focused on the low-frequency atmospheric circulation patterns (SNAO).

2 Data and methods

2.1 Historical flood data

Historical descriptions of flood events are reported in the Alps by local monographies, chronicles, Council minutes, manuscript sources and specialized literature, and from the 18th century on by press and expert reports (Pfister, 1999). Instrumental discharge measurements of gauge stations started in Switzerland mostly at the beginning of the 20th century.

To explain the variability and frequency of floods in Switzerland between 1800 and 2009, an integrated flood damage index (INU) was calculated from two data sources: a flood database, provided by Gees (1997) for the period 1800-1994, which were developed from the historical records compiled by Röthlisberger (1991), Pfister and Hächler (1991) and further historical investigation; and selected flood damage data extracted from the Swiss Flood and Landslide Damage Database of the Swiss Federal Institute for Forest, Snow and Landscape Research, WSL for the period 1972-2009 (Hilker et al., 2009). The contemporary flood series of the WSL, generated from damage events reported by the local, regional and national press and websites (Police, Fire Department, etc.), were transformed according to the database structure of Gees (1997) to extend the flood index.

Both sources (Gees, 1997 and WSL) report the flood damage expressed by the equivalent of present economic loss. In general, the information included in the database is structured as follows: the municipality, river or canton affected by the hazard, the date, the type of process (flood, debris flow, landslide or rockfall), the triggering weather conditions and a description of the damage, including the number of people affected, killed and injured (Hilker et al., 2009). However, the INU considers only flooding, floods and debris flows. Based on this information, we built a database with a matrix structure, A (MxN), where M rows state the event date and each of the N columns reports the flood information for each of the Swiss cantons. The cells from which the matrix is comprised then either bear a code or are left empty depending on the incidence of a flood event on the given date and in the specific canton. The code reports the flood category, based on the damage in Switzerland quantified in millions of Swiss francs (CHF) taking inflation into account (Gees, 1997; Hilker et al., 2009). A flood is considered a low-damage event (L) if the damage is calculated at less than 0.2 million CHF; a medium-damage event (M) if the damage is between 0.2 and 2 million; a severe-damage event (S) if the damage is between 2 and 20 million; a very severe-damage event (VS) if the damage is between 20 and 100 million; and a catastrophic-damage event (C) when the damage caused by the flood event exceeds 100 million CHF.

Difficulties with regard to the homogeneity of historical flood time series are expected due to the lower precision and possible data gaps of flood records from earlier periods. However, Gees (1997) showed that this heterogeneity mostly affects the small and medium category floods, whereas the very severe and catastrophic events do not show this effect since the increased sensibility of the population caused by the increased floods during the first half of the 19th century, the application of the Swiss Federal Law on River Correction since 1854 and the improved information transmission by the press. Moreover, flood mitigation management such as levee construction, retention reservoirs, river detour into large lakes may influence on flood frequency since the 18th century and improved since 1900 (Wetter et al., 2011). Other factors such as ground sealing, canalizing riverbeds and exposure of public infrastructure increase runoff, discharge and economic losses during the 20th century. It is difficult to estimate how these opposite effects partially compensate for each other (Pfister, 1999). It is important to state that the improved river regulation in Switzerland, conducted from 1850 onwards, may mitigate the damage caused by low, medium and major floods, but cannot prevent completely the total impact of category VS and C floods as occurred for example during the 1987 and 2005 events. From our research on flood dynamics and evolution of delta morphology of the Lütschine and Hasli Aare rivers since 1480 (Schulte et al., in preparation), we observe the same trend: the frequency of very severe and catastrophic floods do not show substantial changes, whereas small and medium floods are recorded with improved precision after 1800. Therefore, we use only the very severe (VS) and catastrophic

(C) flood events to generate the flood damage index (INU). To validate the historical flood data, all events of category VS and C in order to build INU index were checked if they were cited by different sources and damage occurred simultaneously in different sites. From 91 events only the event of August, 4th of 1868 were excluded. The flood database of the WSL (1972-2009) is considered as to be complete.

2.2 Instrumental and proxy data

The solar forcing is considered as an external driver of climate dynamics (Stuiver et al., 1997; Versteegh, 2005) and may influence flood frequency (Benito et al., 2003; Schulte et al., 2008, 2012). Average annual sunspot numbers (SN) for the period 1700-2011 were downloaded from the online catalogue of the sunspot index provided by the SIDC-team (World Data Center for the Sunspot Index, Royal Observatory of Belgium, Monthly Report on the International Sunspot Number). To complete this analysis, we used a solar proxy, the annual mean values of the Beryllium-10 records (^{10}Be) measured in the ice core from the NGRIP site in Greenland (Berggren et al., 2009). Deposition of atmospheric ^{10}Be into polar ice sheets is a natural archive with annually resolution about past solar activity and constitutes a proxy for understanding possible connections between the solar variability and the past climate change (Beer et al., 2000; Berggren et al., 2009).

Volcanic eruptions are investigated by mean volcanic sulphate deposition and converted to stratospheric volcanic sulphate injection (in Tg units) for the Northern Hemisphere over the past 200 years (1800-2000). These measures have been extracted from 32 ice core records that cover major part of the Greenland ice sheet (Gao et al., 2008).

Climate variability is analysed from a climate proxy, the annual mean values of the oxygen isotope record $\delta^{18}O$ for the period 1800-1987 from the Greenland ice core GISP 2 (Stuiver and Grootes, 2000). This core provides climate information based on conversion of isotope values to mean annual temperature in Greenland. Furthermore, we determined the average annual temperature for Switzerland from 1800 to 2006 based on data obtained from the EC-project: Multi-centennial climate variability in the Alps (ALP-IMP, 2006). This dataset is based on instrumental data, model simulations and proxy data with the purpose of creating a spatial grid of several climate variables. The average temperature was obtained by calculating the arithmetic mean of the grid points corresponding to Swiss territory.

The low-frequency atmospheric circulation modes were inferred from the daily EMSLP grid taken from the 20th Century V2 Reanalysis Project (20CRP). These data were provided by NOAA/OAR/ESRL PSD, Boulder, Colorado (Compo et al., 2011) and extend the temporal coverage of the NCEP/NCAR Reanalysis Project (Kalnay et al., 1996). The 20CRP is a mission to produce reanalyses of weather maps covering the period from 1871 onwards with a horizontal spatial resolution of 2°. To complete the period covered by the flood data (from 1800 to 2009) and to obtain a continuous time series of low-frequency atmospheric circulation indices, the monthly sea level pressure fields over the North Atlantic and Europe, generated by Luterbacher et al. (2002) for the years 1659-2000, were also integrated. This grid was developed, under the assumption of stationarity in the statistical relationships, using a transfer function based on the combination of early instrumental station series and documentary proxy data from Eurasian sites. The function is derived over the 1901–1990 period and was used to reconstruct the 500-year large scale SLP fields (Luterbacher et al., 2002).

A complete reference list of web links to the different datasets used in the analysis is given at the end of the manuscript.

3 Methods

Given the hydro-climatic differences according to the singular orographic configuration of Switzerland, the trigger processes of floods, especially rainfall generation processes, are different between the northern and southern flank of the Alps (Schmocker-Fackel and Naef, 2010). Although there are several Swiss climatologic and hydrologic regionalization studies (e.g. Kirchhofer, 2000), we conducted a regionalization of the Swiss territory based on a multivariate data analysis. The input data were performed by the matrix of INU (see section 2.1.1). To identify the principal hydro-climatic regions, we applied a Principal Component Analysis (PCA) to the flood matrix in S-mode using the correlation matrix, the scree test to extract the most relevant components and the Equamax rotation for a straightforward interpretation of the model output.

INU is calculated separately for each of the regions determined from the PCA by evaluating the different spatial and temporal patterns that account for the variability in the frequency of floods. The INU is estimated taking a risk (R) approach, whereby the concept of risk (R) is considered to be the product of hazard (P) and vulnerability (V):

$$R = P * V \quad (1)$$

The variable P is estimated from the damage and economic losses caused by floods. The categories of damage are as defined in section 2.1.1. To each category an arbitrary magnitude is attributed: floods classified as VS are given a value of 50, while C floods are assigned a value of 100. Thus, each flood event is defined by a P value that indicates the intensity of the phenomenon. The estimation of V, defined as the spatial distribution of the phenomenon, is based on the number of cantons affected by a flood episode. Finally, by applying equation (1) we obtain an R value for each flood event.

$$R_K = \sum_{i=1}^{m} P_i * V_i \quad (2)$$

K is the flood number (ordinal 1 to N where N is the total number of floods); m is the number of the cantons concerned in the flood number K; Pi is the hazard of the flood number k and the canton i; and V_i is the vulnerability of the flood number K. In our case always $V_i = 1$. The INU is calculated from the integration of all the R values on an annual resolution:

$$INU_{year} = \sum_{i=1}^{j} \sum_{K=1}^{n} R_K \quad (3)$$

INU_{year} is the INU value for a given year; j is the number of the months (1 to 12); n is the number of events in a given month j. Finally, each INU_{year} is standardized, based on the mean and standard deviation, both parameters calculated for the period 1800-2009.

The periodicities of the time series were determined by conducting analyses in the frequency domain. Spectral analysis is a useful tool for examining the information inherent in a time series (Schulz and Statteger, 1997; Schulz and Mudelsee, 2002; Borgmark, 2005). In this study, we used a harmonic analysis to detect periodic signals in the records with presence of noise (Percival and Walden, 1993). The time series were processed using the program SPECTRUM (Schulz and Statteger, 1997), which is based on a periodogram calculated from the Lomb-Scargle Fourier Transform, with a rectangular window, and using a significance level of 0.05 (α=0.05) and a lambda of 0.4 (λ=0.4). This configuration detects a false-alarm level of 99.6% for white noise assessment through the Siegel (Siegel, 1979) test. The red noise spectrum of the records is estimated with the REDFIT software (Schulz and Mudelsee, 2002). This program estimates the autoregressive first-order parameter for unevenly spaced time series and transforms this model into the time domain frequency. To assess, validate and explain the common cyclicities detected in the time series from the harmonic analysis, a cross-spectral analysis (Schulz and Statteger, 1997) was performed using the bivariate spectral analysis module of the program SPECTRUM. This program analyses the coherency and phase spectra to summarize the co-variation of the time series particularly in palaeoclimatic records (Shackleton, 2000).

A further methodology is concerned with the definition of low-frequency atmospheric circulation modes. Several authors use the main EOF calculated from a principal component analysis (PCA) in S-mode applied to the grid of EMSLP using the covariance matrix (Hurrell et al., 2003; Folland et al., 2009; Bladé et al., 2011) and the scree test (Cattell, 1966) to extract the most relevant components without applying any kind of rotation. The analysis was conducted for the domain from 30°N to 70°N and from 30°W to 30°E for the period 1800-2009. To cover the entire period, we used the reconstruction of sea level pressure fields, weighted by the square root of the latitude, over the Eastern North Atlantic and Europe generated by Luterbacher et al. (2002) and the 20CRP (Compo et al., 2011).

4 Results

4.1 Regionalization of Switzerland and INU as a flood damage index

A total of 90 category VS and C floods were recorded in Switzerland in the period 1800-2009.

The regionalization of Switzerland is based on the application of a PCA to the flood matrix. The 2D-plot of the two principal components (not rotated; see Fig. 1a) accounts 22% of the total variance. When the factors are inverted and rotated by 90º, they display approximately the geographic location of the cantons. Two different dynamics related to the principal moisture sources can be inferred from the sample distribution. The Factor 1 is related to a disposition North/South of the cantons, indicating a lower/greater influence of the Mediterranean Sea. The second Factor is explained by West/East cross section suggesting the higher/lower influence of the Atlantic moisture source.

We used the scree-test to extract the most relevant components (see Fig. 1b) and we performed an Equamax rotation in order to achieve the final regionalization of Switzerland considering the two cross sections. The analysis revealed five principal components accounting for 45% of the total variance. Each region is defined by a component (see Fig 1c): the region 1 is composed by the Valais and the western cantons; the region 2 is defined by the western part of the northern slope of the Alps and the western Swiss plateau; the region 3 represents the south-eastern cantons Grisons, Uri and Ticino; the region 4 is the Swiss Jura and the eastern Swiss Plateau; and finally, the region 5 is the eastern part of the northern flank of the Alps. Thus, the rotation improves the division of regions that appear vaguely defined in Fig. 1a. For instance, Uri (UR) marks the transition between the regions 3 and 5 and finally is added to region 3. Moreover, the cantons located in northern and north-western Switzerland, which in Fig. 1a apparently define a single cluster, are split into two areas (region 1 and region 4) after the rotation. This separation distinguishes probably between the flows from the west-northwest and those from the north.

Figure 2 shows the monthly and seasonal distribution of VS and C events for the period 1800-2009. The monthly (Fig. 2a) and seasonal (Fig 2b) flood cycles are heavily pronounced: 65% of these events are concentrated in the summer season (June, July and August), rising to 82% if September is included (extended summer). Furthermore, the monthly distribution presents a peak in August with 37% of all events. It should also be noted that during the months of March, April and December no major floods were recorded. Recall, however, that the flood damage index only considers the events recorded during the high summer months (July and August). We proceed in this way for two main reasons: first, this is the time window considered by the SNAO, which is the principal pattern for explaining rainfall patterns in terms of large-scale atmospheric phenomena; and, second, most of the catastrophic floods (C; 60 %) reported during the time span of this study occurred during this two-month period.

Figure 3a shows the annual flood damage index according to the contribution of each region. The INU captures the high temporal variability of floods showing the alternation of high frequency periods of major flood events and periods of very low frequency or flood gaps. The advantage afforded by the INU is that we are able to process the time series statistically. Figure 3b shows the total annual INU values of the Switzerland and indicates periods with high frequency of flooding (grey shaded). Each column summarizes the information shown in Fig. 3a by using the following expression:

$$INU_{year} = \left(\sum_{i=1}^{N} INU_i \right) \frac{1}{N} \qquad (4)$$

where for a determined year, i is the region number, INU_i is the INU_{year} for the region i and N=5 (total number of regions). Finally, the new data set is normalized by the mean and the standard deviation of the period 1800-2009. The major flood periods can be identified with respect to INU values that exceed the mean plus 1.5 times the standard deviation. The first period marked by a high frequency of major floods (Fig. 3b) extends from 1817 to 1851; the second period from 1881 to 1927, although some flooding did continue to occur, albeit less frequently, up to 1951 (Fig. 3a); the last two periods were recorded from 1977 to 1990 and 2005 to present. Since that date, the 2005 flood event caused the most severe damage (3.1 billion CHF) followed by the 1987 flood (1.77 billion CHF).

4.2 Spectral analysis of large floods

Figure 4a plots the harmonic analysis of the INU undertaken to detect periodicities in the records in the presence of noise (Schulz and Statteger, 1997; Schulz and Mudelsee, 2002; Borgmark, 2005). The analysis identifies periodic signals that are above the 99.6% false-alarm level using the Siegel test, in an interval of frequencies (fs) ranging from 0.005 and 0.011 with a maximum peak at 0.009; at 0.082; between 0.103 and 0.105 with a maximum peak at 0.105; and between 0.391 and 0.413 with a maximum peak at 0.393. A red noise in the signal (Fig. 4b) was not detected. Thus, the harmonic analysis indicates spectral peaks between 92 and 184 years with a maximum spectral peak at 110 years; between 10 and 12 years with a maximum spectral peak at 10 years; and between 2 and 3 years with a maximum spectral peak located at 2 years. In summary, significant spectral peaks were detected around 2 years, 10 years and 110 years. These latter two may correspond, respectively, to the Schwabe (11.04 ± 2.02 years) and Gleissberg cycles (88.6 ± 21 years), such secular periodic processes have been reported in a broad variety of solar, solar–terrestrial, and terrestrial climatic phenomena (Peristykh and Damon, 2003), whereas the first one might correspond to the Quasi-Biennial Oscillation (Baldwin et al., 2001), that it affects the stratospheric flow from pole to pole by modulating the effects of extratropical waves. The spectral analysis therefore seems to provide evidence that solar forcing is a significant factor with regard to the timing of floods in Switzerland.

4.3 Cross-spectral analysis between sunspot numbers and large floods

To compare the periodicities identified in the INU with cycles of solar activity, a harmonic analysis of the annual average sunspot number for the period 1700-2011 was conducted. The results show the main solar cycles on decadal and centennial scales (Fig. 4c) and are consistent with the results of solar periodicities reported by Rogers et al. (2006). The INU shows common periodicities with solar cycles at fs=0.010 and fs=0.090 corresponding to 104 and 11 years, respectively.

To consider the significance of the common spectral peaks of INU and the sunspot record, a cross-spectral analysis was undertaken to obtain the coherency and phase spectra (Fig. 5). Since maximum values in the INU are expected to correlate with minimum solar activity values, as pointed out in a number of studies (e.g. Pfister, 1999; Magny et al., 2003; Schulte et al., 2009a, b), the sign of the INU data was changed prior to cross-spectral analysis to prevent an artificial phase offset by ±180º. The coherency spectrum (Fig. 5a) suggests the presence of periodic components at 104, 22 and 11 years, setting the false-alarm level at α=0.1. The phase spectrum (Fig. 5b) identifies negative angles of -117º ± 20º at fs = 0.010 (104 years), and -98º ± 48º at fs = 0.090 (11 years). These results show that the maximum INU values are related to solar activity minima. However, the angle is positive (132º ± 19º) at fs = 0.045 (22 years). Therefore, the cross-spectral analysis provides evidence that the common and significant periodicities detected in the coherency spectrum at 11 (Schwabe cycle) and 104 years (Gleissberg cycle) are related to a high frequency of flooding and minimum solar activity (negative angles in the phase-spectrum, Fig. 5b), whereas the 22-year cyclicity detected (Hale cycle) is associated with maximum solar activity and a decrease in the flood frequency (positive angles in the phase-spectrum).

4.4 Comparison between modes of low-frequency atmospheric variability and large floods

The INU index provides an excellent tool to explore the space-time dependence between major floods in Switzerland and low-frequency atmospheric circulation patterns. During the high summer, the climate variability in the North Atlantic European sector is synthesized by a major annual variability pattern identified as the SNAO. This pattern was detected by the first covariance eigenvector of EMSLP computed from a PCA in S-Mode, over the domain 30°N-70°N and 30°W-30°E, with a monthly resolution for the two reanalysis grids used: 20CRP (Compo et al., 2011) for the period 1871-2009 (Fig. 6a), and the sea level pressure fields over the North Atlantic and Europe for the period 1659 to 1999 (Luterbacher et al., 2002; Fig. 6b). The low-frequency atmospheric circulation pattern obtained separately from both grids is quite similar, explaining roughly 40% of the EMSLP variance. Both models are comparable to those presented by Folland et al. (2009, see Fig. 1, pp. 1085). Furthermore, the coefficients of the scores matrix report the temporal evolution of the SNAO. The Pearson temporal correlation coefficient between the scores of both time series has a value of 0.89. This level of association has allowed us to create the SNAO index for the period from 1800 to 2009 (see Fig. 6c).

The temporal evolution of SNAO (Fig. 6c) shows three periods dominated by positive phases: the first between 1741 and 1783, the second, more intermittently, between 1867 and 1918, and the third since 1967. The temporal evolution is very similar to that presented by Folland et al. (2009, see Fig. 3, pp. 1087). The second and third phases coincide with the last three phases of high frequency flooding in Switzerland. In addition, the positive phase of SNAO detected in the 18th century coincides with the flood cluster between 1740 and 1790 reconstructed by Schmocker-Fackel and Naef (2010b). Only the high frequency phase of major floods that was recorded during the first half of the 19^{th} century (cf. Fig. 3b) is not reflected in the temporal evolution of the SNAO data.

The increase in flood frequency occurs mostly in positive phases in the large-scale circulation pattern for the high summer period. Flood events with INU>5 SD (Fig. 7a) correlate with positive SNAO values (Pearson's temporal correlation coefficient is 0.45, significant at the 95% confidence level). However, the study of the complete amplitude of the INU and SNAO signals (Fig. 7b) indicates a second flood pattern during negative phases of SNAO. Table 1 shows the mean values of SNAO for the years assigned to four categories of the INU whose thresholds were defined according to the standard deviation (from INU>0 SD for at least one major flood to INU>5 SD for highest flood impacts). The 33 summers with very severe or catastrophic floods in Switzerland (INU>0 SD) show a weak positive value of SNAO = 0.04 (± 0.90), which increases to 0.45 (± 0.90) when considering only those summers that have registered a flood with a large impact (INU>5 SD). The number of years involved in INU>0 with positive phase of SNAO is also higher than the years associated with a negative phase (20 and 13, respectively), noting that the four years involved in the major floods have all of them a positive value of SNAO. However, with regard to a reliable explanation of the triggering processes for floods in Switzerland which are based on large-scale atmospheric patterns, we also observe a significant number of years in negative SNAO phase. In addition, this is shown by the 2^{nd} percentile (see Table 1) indicating negative values of SNAO up to

INU>2.5 SD. In the sections 5.1 and 5.4 we focus on the issue if the observed differences in the behaviour of the positive and negative SNAO phases are linked to the two spatial patterns associated with the hydro-climatic regionalization (see Section 5.1 and Fig. 8). Moreover, we briefly analyse whether there have been changes in atmospheric circulation patterns associated with major floods during the last two hundred years.

5 Discussion

5.1 Hydro-climatic regionalization and flood periods in Switzerland

The hydro-climatic regionalization performed by the PCA shows two patterns of spatial variability related to the two principal moisture sources that affect Switzerland: Mediterranean and Atlantic humidity supplies. The first pattern is related to the North-South cross section while the second pattern is defined by the West-East cross section (see Fig. 1a). Taking into account these findings, the final classification presents five different regions (see Fig. 1b and Fig. 1c). The two cross sections stress the regionalization based on the INU index. The three physiographic units, the Jura, Swiss Plateau and Alps are related to different sources of humidity. The northern slope of the Alps and the Swiss Plateau are divided into three regions linked to the proximity to the Atlantic fluxes. In addition, the region 2 (particularly the Bernese Alps) marks the intersection of both patterns: on one hand the Atlantic flux and on the other hand the moist Mediterranean air masses that flow across the Alps and encounter the cooler Atlantic air at the northern Alpine slope (Pfister, 1999).

The regional distribution is consistent to other classifications of Switzerland (e.g. Kirchhofer, 2000) that have been widely used such as for weather forecast and warnings for heavy rain (Schmocker-Fackel, 2010a). A major drawback of our classification is that regions have been constructed from administrative units (cantons) that in some cases may include different physiographic units. For example region 2 includes the canton Berne which range from the northern Alps to the Swiss plateau and the southern slopes of the Jura Massif. However, the classification avoids the overestimation of the small Swiss cantons.

The temporal evolution of the regional INU shown in Fig. 8 indicates two spatial flood patterns: during phase A from 1820 to 1910 flood numbers increased in the basins of the west and northern flank of the Alps (region 1, 4 and 5), whereas during phase B from 1970 to the present floods increased in the centre and south of the Alps (regions 2 and 3). This decadal variability might be linked to changes in patterns of extreme precipitation and large-scale atmospheric circulation (Frei et al., 2000). Schmocker-Fackel and Naef (2010a) suggest that this changing atmospheric pattern is not well defined for Switzerland yet.

The total INU index, summarizing the temporal distribution of the frequency of very severe and catastrophic floods in Switzerland, presents four mayor flood periods: the first extends from 1817 to 1851, the second from 1881 to 1927, the third encompasses 1977 to 1990 and the fourth was initiated in 2005 (Fig. 3b and 9). These periods largely coincide with those reported in other studies for Switzerland (Hächler-Tanner, 1991; Röthlisberger, 1991; Gees, 1997; Pfister, 1999; Schmocker-Fackel and Naef, 2010b) and, furthermore, with the periods identified in Spain, Italy and the Czech Republic (Barriendos and Rodrigo, 2006; Camuffo and Enzi, 1996; Brázdil et al., 2006). Our study shows that periods of high frequency flooding have a period around 90 years. This range is very similar to that observed in Germany: for instance, Glaser and Stangl (2004) report flood clusters that range between 30 and 100 years during the last millennium, whereas in northern Switzerland these periods have a duration of between 30 and 120 years (Schmocker-Fackel and Naef, 2010b). In our opinion, the INU provides a robust index, which captures the variability in major flood frequency, although the distribution of the clusters is not homogeneous in time.

Pfister (1999) who reconstructed the floods of the Rhine, Rhone and Reuss rivers and of Lake Maggiore from documentary sources and instrumental data for the past 500 years found that major flood clusters occurred during cold periods of the Little Ice Age. The last flood pulse from 1827 to 1875 corresponds to the first period identified in our study (1817-1851). However, the Little Ice Age also included periods with no flood activity in alpine basins and which coincided with periods of decreased solar activity, such as the Maunder Minimum (Pfister, 1999). As for the flood analysis undertaken by Schmocker-Fackel and Naef (2010b) in Swiss catchments, the alternation of periods of high and low flood frequencies coincides with those reported in our study.

The single high flood frequency period between 1820 and 1940 identified by Schmocker-Fackel and Naef (2010b) appears in our INU index as two flood pulses separated by a short flood gap (1851-1881; Fig. 3b). The results compiled by Pfister (1999) from the Rhone, Reuss/Linth and Alpenrhein basins show a high flood frequency from 1860 to 1875. This discrepancy can be explained in part by the different statistical processing methods applied to the flood data categories and by differences in the number of catchments studied (number of samples). In addition, the INU index only considers the very severe and catastrophic floods that occurred during the high summer months (July and August), whereas Pfister (1999) includes the total number of events in all seasons. However, all authors (Röthlisberger, 1991; Gees, 1997; Pfister, 1999) rule out any possible data incompleteness with regard to very severe and catastrophic floods on the grounds that the local press and administration paid considerable attention to extreme hydrological events following the application of the Swiss federal law providing for river correction subsidies in 1848. However, there is a consensus in the literature that the older the event (and, hence, the associated damage) is, the less clear is the definition of the thresholds between the loss categories.

A second flood gap is recorded from 1944-1972 by the INU reflecting the absence of extreme weather conditions (predominance of negative SNAO; Fig. 6c) that might trigger major floods. Pfister (1999) argues that anthropogenic influence (land use, deforestation) in the major floods is not the dominant driving factor, but rather the long-term summer precipitation minima between 1935 and 1975. According to Gees (1997), river regulation, and the building of embankments and reservoirs substantially reduced the damage caused by smaller and medium floods after 1854, whereas the mitigation of the impact of very severe and catastrophic floods showed only limited success, particularly in the upper alpine catchments. Nevertheless, the more intensive land use in former flood areas protected by river embankments contributed to increased losses (Gees, 1997). Moreover, it is important to bear in mind that the general increase in population, exposure values (due to the increase in the Gross Domestic Product) and urban agglomeration (e.g. Zurich) have contributed to higher flood damage indices, particularly in recent decades. A decrease in the number of floods is also reported by Schmocker-Fackel and Naef (2010b) for northern Switzerland between 1940 and 1970, and Wetter et al. (2011) observe a period of very low frequency flooding in the city of Basel (Rhine river) for the period 1877-1999 and in Lindau (Lake Constance) for the 1910-1999 time interval.

Finally, the increase in flood events since 1977 recorded by the INU seems to result from both increasing vulnerability and from changes in the climate signal. With regard to this first factor, Glaser et al. (2010) found that even though the number of extreme hydrological events decreased with respect to the 19th century, estimations of overall losses are substantially higher. This is related to the increased vulnerability and exposure values in flood prone areas as a consequence of the expansion of urban areas. As for the influence of climate variability on flooding in recent decades, Knox (2000) stated that the unusually high frequencies of large floods observed in many regions since the early 1950s occurred during a period of global temperature increase and that the occurrence of extreme floods during the Holocene is often associated with rapid climate changes. In Switzerland, the flood frequency in many basins has increased since the 1970s (Gees, 1997; Pfister, 1999). However, Schmocker-Fackel and Naef (2010a) consider that the flood frequencies observed during the past four decades do not exceed the range recorded during the last five centuries.

5.2 Possible control of solar variability

In recent decades the sun-climate relation has come under analysis (Solanki and Fligge, 2000; Versteegh, 2005; Gray et al. 2005) with the solar variability being proposed as a possible driving force of flood events (Benito et al., 2003; Vaquero, 2004). Schulte et al. (2008, 2009a, 2014) consider the impact of solar activity on the regional hydrological regime (e.g. Gleissberg cycle) to have been one of the main factors triggering the major floods in the Lütschine and Lombach catchments in Switzerland over the last 3,200 years.

By undertaking spectral analyses of the INU and the sedimentary proxies of the northern slopes of the Alps (Schulte et al., 2014), we are able to identify common flood cycles with a variation ranging between 70 and 150 years. The periodicities of so-called "100-year events" (according to Glaser et al., 2010) could be explained by centennial-scale solar cycles, which have also been identified in other sedimentary records, including those in eastern France, Switzerland, Netherlands, the UK, Spain and California (see, for example, Magny et al., 2003; Versteegh, 2005). Cross-spectral analysis between the INU and sunspot numbers suggests that the common and significant periodicities detected in the coherency spectrum of 11 (Schwabe cycle) and 100 years (Gleissberg cycle) coincide with the relation between a high flooding frequency and minimum solar activity (negative angles in the phase spectrum). This fact is supported by the findings of Wirth et al. (2013a) in the reconstruction of the summer floods in the Southern European Alps. Furthermore, the 22-year cyclicity detected (Hale cycle) includes the link between solar activity maxima and decreased flood frequency (positive angles in the phase spectrum). This bi-decadal frequency of the INU "flood minima" is confirmed by climate proxies in the western United States where droughts occurred with a 22-year periodicity from 1700 onwards (Cook and Stockton, 1997; Briffa, 2000).

5.3 Short-term external forcing on flooding

To evaluate possible links between flooding and short-term external forcing fluctuations, the volcanic eruptions, SNAO, $\delta^{18}O$, ^{10}Be and sunspot number have been plotted alongside the INU index for Switzerland (Fig. 9). All the proxy series are plotted as normalized values smoothed with an 11-year low-pass Gaussian filter, except the sunspot number record smoothed with a 22-year filter while volcanic eruptions and INU time series are not filtered. It should be noted that the links with solar and climate proxies can generate two types of problem: first, the time lags between sunspot numbers (SN), production and the deposition of ^{10}Be (1-2 years) and $\delta^{18}O$ (from years to decades; e.g. the reconstructed time lags between ^{14}C and $\delta^{18}O$ records during the Wolf and Maunder Minimum rise up to 40 years; Stuiver et al., 1997; Vonmoos et al., 2006; Abreu et al., 2012) in the natural archives have to be considered; and, second, the significance of the signal of the palaeoclimate proxies at the regional and global scale has to be interpreted. Despite these uncertainties, comparison of ^{10}Be concentration, sunspot numbers and temperature records from Greenland ice shows fairly good correlation since the 17th century (Stuiver et al., 1995; Beer et al., 2000). However, other proxies such as the $\delta^{18}O$ are influenced by the oceanic thermohaline circulation besides the solar activity. However, it must be taken into account that the length of INU time series is relative short, covering 200 years, and linkages are based on only four flood periods and three flood gaps. Therefore, the relation between INU and the different climate proxies must be interpreted with caution and simple associations must not explain causal mechanism. Furthermore, it should be stressed that the INU signal includes uncertainties due to the integration of natural and anthropogenic variables. These reasons have to be borne in mind before discussing the following results.

Three periods of low solar activity (low number of sunspots, positive anomalies of ^{10}Be) have been recorded during the last 200 years (Fig. 9; *cf.* Solanki and Fligge, 2000; Berggren et al., 2009): the first period covers the years leading up to 1840, and corresponds to the final stages of the Dalton Minimum; the second period lasts from 1880 to 1910 (^{10}Be) and 1935 (SN), corresponding to the solar minimum of 1900; and a third period begins after 2005 reaching minimum values in 2009. Figure 9 provides evidence that the periods marked by a high flood frequency typically correspond to periods characterized by a predominance of positive ^{10}Be anomalies and, therefore, associated with episodes of low solar activity. This pattern was particularly strong during the solar minimum of 1900. The period of high flood frequency between 1817 and 1855 largely corresponds to a period characterized by positive ^{10}Be anomalies, although the flood peaks occurred in the transition between a solar minimum and a solar maximum. During this period an extra cooling occurred which was associated with the eruption of Tambora (1814) plus two eruptions in the years 1831 and 1835 (Fig. 9). Considering both forcings (solar and volcanic), the temperature anomaly for this period compared to the 1961–1990 mean was around -0.5 °C in the Northern Hemisphere (Gao et al., 2008) and -1.1 ºC for the Swiss Alps (Büntgen et al. 2006). Finally, the maximum of the last flood cluster corresponds to a short period of low solar activity after 2005.

Several authors (Pfister, 1999; Knox, 2000; Magny et al., 2003; Benito et al., 2003; Schulte et al., 2012; Ortega and Garzón, 2009) contend that the most significant variations in the frequency of flooding have occurred during cold climate phases, particularly during transitional stages of climatic pulses. This pattern has also been observed in Switzerland during the last 500 years (Schmocker-Fackel and Naef, 2010b; Glur et al., 2013; Wirth et al., 2013a, 2013b), although after the 1970s the climate and flood pattern changed. The $\delta^{18}O$ record GISP2 from Greenland (Stuiver and Grootes, 2000), influenced by North Atlantic dynamics, provides a proxy of the temperature variability in the middle and high latitudes of the northern hemisphere. The peak clusters of the flood damage index INU (Fig. 9) can be related to periods dominated by negative $\delta^{18}O$ anomalies (bearing in mind that the axis is inverted), principally to the cooler pulses from 1830 – 1845, from 1880 – 1930 and during the 1980s.

To corroborate these results obtained from large-scale proxies, in Fig. 10 we plotted the normalized annual average temperature of Switzerland for the period 1800-2009 versus the INU. The first two flood clusters occurred during a period of negative temperature anomalies between 1825 and 1935. In addition, these two flood clusters are related to pulses of marked temperature decreases separated by a flood gap which corresponds to a period of temperature recovery (slightly negative temperature anomalies >-0.2ºC) and solar activity (Fig. 9). The flood peak of summer 1987 occurs in a period in which temperature anomalies in Switzerland were slightly positive, but $\delta^{18}O$ was negative in Greenland, indicative as such of the influence of North Atlantic dynamics. The 2005 and 2007 floods occurred in a clearly warm phase in Switzerland, corresponding to a contemporary maximum. However, the climatic interpretation of these events should be undertaken with caution because the final temperature data once again present a slight fall and sunspot numbers clearly decrease. Yet, these data represent the end of the time series. As for the pattern of flood gaps, Fig. 10 provides clear evidence: gaps of floods (1852-1880; 1928-1976) are related to positive temperature trends. Moreover, the contemporary flood cluster is divided by the positive trend towards the temperature maximum.

From the analyses of the various proxies, we infer that periods of decreased solar activity and low-frequency cold climate pulses ($\delta^{18}O$) have a significant impact on major summer floods in Switzerland. Nevertheless, the non-linear pattern of flood occurrences (e.g. since 1977) needs to be related to the complex relationship between exogenic, endogenic and autogenic climate forcing mechanisms. Therefore, hemispheric or global changes that occur in the atmospheric general circulation or in ocean currents and that affect storm tracks and air mass limits (Hirschboeck, 1988; Knox, 2000) should be considered when investigating periods of high flood frequency.

The summer climate in western Europe can be synthesized by the SNAO and we have identified a qualitative relationship between the SNAO and the summer flood damage index INU (section 3.4). Figure 9 shows that the second, third and fourth clusters of major floods in Switzerland coincide mostly with positive phases of SNAO, whereas the first flood cluster is not in phase with this atmospheric circulation pattern. However, we suggest that the origin of the flood clusters might be attributed to the location of the atmospheric action centers during the positive (or negative) phase. The variability of the SNAO pattern is associated with changes in the storm track of the North Atlantic European sector. Positive (negative) values of SNAO are related to the northward (or southward) shift of the storms and thus they become stronger over Iceland and the Norwegian Sea during a positive phase and weaken towards the south. This pattern generates dry, warm weather, especially in central and western Europe due to strong anticyclonic conditions (Folland et al., 2009). In southern Europe, the climate becomes more humid during these positive phases (Bladé et al., 2011). This atmospheric dynamics is illustrated in Fig. 6. We should emphasize that negative anomalies are observed in lower and middle atmospheric levels over the Mediterranean area. Switzerland lies on the northern boundary of this negative domain. This pattern promotes atmospheric instability in these areas and leads to positive precipitation anomalies. The enhanced precipitation is related to the presence of a strong upper level trough over the south-west of the Iberian Peninsula and the Mediterranean area that generates a cooling of the air in middle atmospheric levels and an increased potential for instability. Thus, SNAO acts as a major control of climate variability during the high summer, not only in north-western Europe, but also in southern areas (Bladé et al., 2011). In this sense, this explains the qualitative link between the high summer large-scale circulation pattern and the frequency of major flooding in Switzerland. Additionally, the analysis of the different categories of the INU in relation to SNAO (Table 1) shows that the positive phase of the pattern explains large impact flood events (INU >5 SD; 4 of 33 episodes), but only part of the variability of the signal of INU (20 of 33 events). By contrast, the negative phase of SNAO is associated with the remaining 11 events.

5.4 Summer North Atlantic Oscillation and flood variability

Based on the relationship between the North Atlantic Dynamics and the INU index, two patterns might be proposed to explain the flooding in Swiss catchments since 1800.

The first flood pattern is associated with positive SNAO phases (mean values vary between 0.04 and 0.45; Table 1; see Figure 11). The INU >5 SD category includes the four most catastrophic floods that affected Switzerland in the last 200 years: 1831, 1834, 1846, and 2005. These events occurred during periods of low solar activity (positive values of ^{10}Be) and, with the exception of the 2005 flood, during episodes of cold climate pulses in Greenland (negative values of δ^{18}O) and in the north-western Alps (temperature anomalies; Fig. 9 and 10). During these cold pulses the accumulation of snow and ice in the headwaters is significant, increasing the flood risk during warm years when melting processes contribute markedly to summer discharge. This flood pattern occurs in years dominated by positive SNAO phases when depressions are usually associated with the Atlantic cyclones that become more intense over the Mediterranean Sea, and follow a northeast to north-northeast track over the Alps (Blöschl et al. 2013). This path is known as Vb (van Bebber, 1891) and produces long-lasting, intense rainfall due to (1) the high water vapour content from the Mediterranean, (2) the orographic uplift of air masses and (3) the reinforcement suffered by negative anomalies of temperature and geopotential height that occurs at the lower and middle levels of the atmosphere. The most affected regions in Switzerland are the Regions 2 (western part of the northern flank of the Alps), 3 (Grisons plus southern flank of the Alps) and 5 (eastern part of the northern flank of the Alps) that accounts for the 70% of the total of floods with INU >2.5 and SNAO in positive phase (see Fig. 11). Similar findings have been reported by Grebner (1997) and Pfister (1999). They report that this atmospheric configuration causes catastrophic floods, especially in the greater Alpine region. Mudelsee et al. (2004) applied for the summer flooding of the river Oder and Elbe in eastern central Europe a point-wise biserial correlation coefficient between the flood events and sea level pressure and the 500 hPa geopotential height; obtaining a pattern that is very similar to the large-scale atmospheric circulation mode of positive SNAO proposed herein. Müller and Kaspar (2011) obtained similar results for the summer floods in the Mura and Drava (south-eastern Alps) catchments, typical transboundary rivers of the eastern slopes of the Alps. The floods in these rivers were frequently connected with moisture fluxes from the east or the north at the 850 hPa level. This configuration is associated with cyclones that are intensified over the Mediterranean Sea that affect central Europe as they move to the north-east along the Vb track. These results are also in agreement with the findings reported by Schmocker-Fackel and Naef (2010b) to the effect that the periods of high flood frequency in Switzerland are in phase with the summer floods of the Czech Republic (Brázdil et al., 2006), Italy (Camuffo and Enzi, 1996) and the eastern half of the Iberian Peninsula (Barriendos and Rodrigo, 2006), while the relationship is not so significant when compared with the flood occurrences observed in Germany (Glaser and Stangl, 2004).

The second flood pattern is determined by INU-values linked to periods of low solar activity (positive values of ^{10}Be) and episodes that are climatically cold (negative values of δ^{18}O), but unlike the first pattern, the SNAO is in the negative phase. The number of years related to INU>0 is less than the pattern described above (13 of 33 events) and it is noteworthy that there are no SNAO negative values for the category of INU> 5. The synoptic configurations related to this large-scale atmospheric circulation mode (Fig. 12) are characterized by cold fronts originating over the Atlantic, tracing a northwest to southeast path, funnelled by a low located at the latitude of Scandinavia and a high over the Atlantic Ocean. This configuration is very similar to that of the synoptic patterns defined by Jacobeit et al. (2006) and which are associated with the large summer floods in eight central European catchments (Rhine, Main, Mosel, Danube, Weser, Elbe, Spree and Oder). The persistence of this situation produces significant rainfall over Switzerland and, consequently, floods that can have a considerably detrimental impact on the territory, its property and people (Pfister, 1999). The most affected regions in Switzerland are the Regions 2 (western part of the northern flank of the Alps) and 4 (eastern Jura mountains and Swiss Plateau) that accounts for the 62% of the total of floods with INU >2.5 and SNAO in negative phase (see Fig. 12).

Thus, the SNAO defines the sensitivity of the Swiss river systems to extreme hydrological events controlled by the atmospheric processes operating in the Mediterranean area (disturbance over the Gulfs of Genoa and Venice) and in the North Atlantic (cold fronts channelled between the Scandinavian low and the Atlantic anticyclone). Finally, the series shows differences and changes in the temporal and spatial distribution of floods numbers (see Fig. 8) and related phases of SNAO (see Fig. 11 and 12). We have evidences that the positive phase of SNAO strongly influences the floods in central, eastern and southern Switzerland, while the negative phase affects the central, western and northern Switzerland. From Fig. 8, we can infer a spatial flood pattern for the late pulses of the Little Ice Age (Phase A, cool period) which mainly affects the northern and western part of Switzerland, while a second pattern influences the central and southern part during the last four decades of the period of study (Phase B, warm period). From this spatial distribution of floods, it is possible to identify a change of the atmospheric patterns that affects the frequencies of floods in Switzerland during the last two hundred years: the Summer North Atlantic Oscillation persists in negative phase during the last cool pulses of the Little Ice Age (1817-1851 and 1881-1927 flood clusters), whereas the positive phases of SNAO prevail during warmer climate of the last four decades (flood clusters from 1977 to present). These findings are consistent with the trend of the SNAO time series for the period 1800-2009 (see Fig. 6; Mann-Kendall trend test shows a significant and positive trend at a 95% confidence level). Based on the obtained results, future research should focus on how these atmospheric mechanisms control the onset of high frequency periods of major flooding.

6 Conclusions

We presented a new flood damage index (INU) for Switzerland between 1800-2009 exploring the influence of external forcings on flood frequencies and links with the Summer North Atlantic Oscillation (SNAO). Our major findings are presented below.

1. The hydro-climatic regionalization shows two patterns of spatial variability related to the principal moisture sources that affect Switzerland: Mediterranean and Atlantic humidity supplies. The first pattern is defined by a North-South cross section, while the second is linked to a West-East cross section. Taking into account these findings, the final classification presents five different regions that are consistent to other hydrographic classifications developed for Switzerland.
2. Despite regional climate differences within Switzerland, INU provides evidence that the 1817-1851, 1881-1927, 1977-1990 and 2005-present flood clusters are mostly in

phase with palaeoclimate proxies and North Atlantic dynamics. Moreover, these periods coincide with those identified in a range of studies concerned with the occurrence of floods in Switzerland and in the other river systems of eastern central Europe. The 20th century flood gap identified by the INU, reflecting the absence of extreme weather conditions, contrasts with the higher flood frequency of the last three to four decades, which has contributed to the increased perception of flood events.

3. The cross-spectral analysis shows that the periodicities detected in the coherency and phase spectra of 11 (Schwabe cycle) and 104 years (Gleissberg cycle) are related to a high flooding frequency and solar activity minima, whereas the 22-year cyclicity detected (Hale cycle) is associated with solar activity maxima and a decrease in flood frequency. We suggest that changes in large-scale atmospheric circulation (autogenic forcing) and solar activity (exogenic forcing) influence the occurrence of flood periods, although there is no general consensus as to how solar forcing has affected climate and flood dynamics in recent centuries.

4. The analysis of the modes of low-frequency atmospheric variability based on the standardized daily anomalies of sea level pressure shows that Switzerland is located close to the border between different modes of summer atmospheric circulation that are controlled by North Atlantic dynamics. Small shifts of this system border may introduce atmospherical instability over the Swiss river catchments. Very severe and catastrophic flood episodes are influenced strongly by positive (mostly central and southern basins) and negative SNAO (mostly the northern basins) mode, which include a range of synoptic patterns that generate severe floods. Finally we can state that the SNAO in negative phase controlled notably major floods during the last stages of the Little Ice Age (1817-1851 and 1881-1927 flood clusters), while the positive SNAO prevailed during last four warmer decades (flood clusters from 1977 to present).

Acknowledgements

The work of the Fluvalps Research Group (PaleoRisk; 2014 SGR 507) was funded by the Catalan Institution for Research and Advanced Studies (ICREA Academia 2011) and the Spanish Ministry of Education and Science (CGL2009-0111; CGL2013-43716-R). The flood damage data for the period 1972-2010 were provided by the Swiss Federal Institute for

Forest, Snow and Landscape Research WSL (Swiss flood and landslide damage database). The authors wish to thank the SIDC-team, the World Data Center for the Sunspot Index of the Royal Observatory of Belgium and the ALP-IMP project for the Annual Temperature of Switzerland. The authors are also grateful to the DOE INCITE program, the Office of Biological and Environmental Research (BER) and to the NOAA, which provided the Twentieth Century Reanalysis Project dataset. The authors thank Nadine Hilker for preparation of flood damage data (1972-2009) and Norina Andres for her helpful comments. We thank the two anonymous referees for useful comments and suggestions on improving the manuscript.

References

Abreu, J.A., Beer, J., Steinhilber, F., Christl, M., Kubik, P.W.: ^{10}Be in Ice Cores and 14C in Tree Rings: Separation of Production and Climate Effects, Space Sci. Rev., 176 (1-4), 343-349, 2012.

ALP-IMP: Multi-centennial climate variability in the Alps based on Instrumental data, Model simulations and Proxy data. Final report for RTD-project ALP-IMP (EVK-CT-2002-00148). 2006.

Baldwin, M.P., Gray, L.J., Dunkerton, T.J., Hamilton, K., Haynes, P.H., Randel, W.J, Holton, J.R., Alexander, M.J., Hirota, I., Horinouchi, T., Jones, D.B.A., Kinnersley, J.S., Marquardt C., Sato, K., Takahashi, M.: The Quasi-Biennial Oscillation, Rev. Geophys., 39 (2), 179-229, 2001.

Barriendos, M., Rodrigo, F.S.: Study of historical flood events on Spanish rivers using documentary data, Hydrol. Sci. J., 51, 765-783, 2006.

Beer, J., Mende, W., Stellmacher, R.: The role of the sun in climate forcing, Quaternary Sci. Rev., 19, 403-415, 2000.

Benito, G., Díez-Herrero, A., de Villalta, M.: Magnitude and frequency of flooding in the Tagus River (Central Spain) over the last millennium, Climatic Change, 58 (1-2), 171-192, 2003.

Benito, G., Ouarda, T.B.M.J., Bárdossy, A.: Applications of Palaeoflood hydrology and historical data in flood risk analysis. In: Benito, G., Ouarda, T.B.M.J., Bárdossy, A. (Eds.), Palaeofloods, historical data and climate variability, J. Hydrol., 313 (1-2), 1-2, 2005.

Berggren, A.M., Beer, J., Possnert, G., Aldahan, A., Kubik, P., Christl, M., Johnsen, S.J., Abreu, J., Vinther. B.M.: A 600-year annual ^{10}Be record from the NGRIP ice core, Greenland, Geophysical Research Letters 36, L11801. DOI: 10.1029/2009GL038004, 2009

Bladé, I., Liebmann, B., Fortuny, D., Geert Jan van Oldenborgh.: Observed and simulated impacts of the summer NAO in Europe: Implications for projected drying in the Mediterranean region, Clim. Dyn., 39 (3-4), 709-727, 2011.

Boch, R., Spötl, C.: The origin of lamination in stalagmites from Katerloch Cave, Austria: Towards a seasonality proxy, PAGES News, 16 (3), 21-22, 2008.

Blöschl, G., Nester, J., Komma, T., Parajka, J., Perdigão R.: The June 2013 flood in the Upper Danube Basin, and comparisons with the 2002, 1954 and 1899 floods, Hydrol. Earth Syst. Sci., 17, 5197–5212, 2013.

Borgmark, A.: Holocene climate variability and periodicities in south-central Sweden, as interpreted from peat humification analysis, The Holocene, 15 (3), 387-395, 2005.

Brázdil, R., Dobrovolný, P., Kakos, V., Kotyza, O.: Historical and recent floods in the Czech Republic. Causes, seasonality, trends, impacts. In: Schanze, J., Zeman, E., Marsalek, J. (Eds.), Floods risk management. Hazards, vulnerability and mitigation measures, NATO Science Series, Springer-Verlag, Berlin, pp. 247-259, 2006.

Briffa, K.R.: Annual climate variability in the Holocene: interpreting the message of ancient trees, Quaternary Sci. Rev., 19, 87-105, 2000.

Büntgen, U., Frank, D., Nievergelt, D., Esper, J.: Summer temperature variations in the European Alps, A.D. 755-2004, J. Climate, 19, 5606-5623, 2006.

Burger, L.: Informationsbeschaffung bei Hochwassersituationen – Dokumentation der grössten überregionalen Hochwasserkatastrophen der letzten 200 Jahre in der Schweiz, Diplomarbeit, Bern, 2008.

Camuffo, D., Enzi, S.: The analysis of two bi-millennial series. Tiber and Po river floods. In: Jones, P.D., Bradley, R.S. and Jourzel, J. (Eds.), Climate variations and forcing mechanisms of the last 2000 years, NATO Science Series, Springer-Verlag, Berlin 141, pp. 433-450, 1996.

Casty, C., Wanner, H., Luterbacher, J., Esper, J., Böhm, R.: Temperature and precipitation variability in the European Alps since 1500, Int. J. Climatol., 25 (14), 1855-1880, 2005.

Cattell, R.B.: The scree test for the number of the factors, Multivar. Behav. Res., 1, 245-276, 1966

Compo, G.P., Whitaker, J.S., Sardeshmukh, P.D., Matsui, N., Allan, R.J., Yin, X., Gleason, B.E., Vose, R.S., Rutledge, G., Bessemoulin, P., Brönnimann, S., Brunet, M., Crouthamel, R.I., Grant, A.N., Groisman, P.Y., Jones, P.D., Kruk, M., Kruger, A.C., Marshall, G.J., Maugeri, M., Mok, H.Y., Nordli, Ø., Ross, T.F., Trigo, R.M., Wang, X.L., Woodruff, S.D., Worley, S.J.: The Twentieth Century Reanalysis Project, Q. J. Roy. Meteor. Soc., 137, 1-28, 2011.

Cook, E.R, Stockton, C. W.: A new assessment of possible solar and lunar forcing of the bidecadal drought rhythm in the western United States, J. Climate, 10, 1343-1356, 1997.

Folland, C.K., Knight, J., Linderholm, H.W., Fereday, D., Ineson, S., Hurrell, J.W.: The summer North Atlantic Oscillation: past, present, and future, J. Climate, 22, 1082-1103, 2009.

Frei, C., Davis, H.C., Gurtz, J., Schär, C.: Climate dynamics and extreme precipitation and flood events in central Europe, Intergraded Assessment, 1, 281–299, 2001.

Gees, A.: Analyse historischer und seltener Hochwasser in der Schweiz. Bedeutung für das Bemessungshochwasser, Geographica Bernensia G53, Bern, Switzerland, 1997.

Glaser, R., Stangl, H.: Climate and floods in Central Europe since AD 1000: Data, methods, results and consequences, Surv. Geophys., 25 (5-6), 485-510, 2004.

Glaser, R., Riemann, D., Schönbein, J., Barriendos, M., Brazdil, R., Bertolin, C., Camuffo, D., Deutsch, M., Dobrovolný, P., van Engelen, A., Enzi, S., Halíčková. M., Koenig, S.J., Kotyza, O., Limanówka, D., Macková, J., Sghedoni, M., Martin, B., Himmelsbach, I.: The variability of European floods since AD1500, Climatic Change 101 (1), 235-256, 2010.

Gao, Ch., Robock, A., Ammann, C.: Volcanic forcing of climate over the past 1500 years: An improved ice-core-based index for climate models, J. Geophys. Res., 113, D23111, doi: 10.1029/2008JD010239, 2008.

Glur, L., With, S., Büntgen, U., Gili, A., Haug, G., Schär, Ch., Beer, J., Anselmetti, F.: Frequent floods in the Europeans Alps coincide with cooler periods of the past 2500 years, Scientific Reports, 3: 2770, doi: 10.1038/srep2770, 2013.

Gray, L. J., Beer, J., Geller, M., Haigh, J. D., Lockwood, M., Matthes, K., Cubasch, U., Fleitmann, D., Harrison, G., Hood, L., Luterbacher, J., Meehl, G. A., Shindell, D., van Geel B., White W.: Solar influences on climate, Rev. Geophys., 48, RG4001, doi: 10.1029/2009RG000282, 2010

Grebner, D.: Meteorologische Verhältnisse und Starkniederschläge im Alpenraum. In: Recherche dans le domaine des barrages, Crues extrêmes, Laboratoire de constructions hydrauliques, Département d'ingénierie civil. Séminaire à l'Ecole Polytechnique Fédérale de Lausanne, Communication 5, 1-6, 1997.

Hächler-Tanner, S.: Hochwasserereignisse im Schweizerischen Alpenraum seit dem Spätmittelalter, Raum-zeitliche Rekonstruktion und gesellschaftliche Reaktionen, Lizenziatsarbeit in Schweizergeschichte, Historisches Institut der Uni Bern, 1991.

Hilker, N., Badoux, A., Hegg, C.: The Swiss flood and landslide damage database 1972-2007, Nat. Hazards Earth Syst. Sci., 9, 913-925, 2009.

Hirschboeck, K.K.: Flood hydroclimatology. In: Baker, V.R., Kochel, R.C., Patton, C. (Eds.), Flood Geomorphology, John Wiley, pp. 27-49, 1988.

Holzhauser, H., Magny, M., Zumbühl, H.J.: Glacier and lake-level variations in west-central Europe over the last 3500 years, The Holocene, 15 (6), 789-801, 2005.

Hurrell, J.W., Kushnir, Y., Ottersen, G., Visbeck, M.: An overview of the North Atlantic Oscillation. In: Hurrell, J.W., Kushnir, Y., Ottersen, G. and Visbeck, M. (Eds.), The North Atlantic Oscillation: climatic significance and environmental impact, Geophysical Monograph Series, 134, 1-35, 2003.

Jacobeit, J., Philipp, A., Nonnenmacher, M.: Atmospheric circulation dynamics linked with prominent discharge events in Central Europe, Hydrolog. Sci. J., 51, 946-965, 2006.

Kalnay, E., Kanamitsu, M., Kistler, R., Collins, W., Deaven, D., Gandin, L., Iredell, M., Saha, S., White, G., Woollen, J., Zhu, Y., Chelliah, M., Ebisuzaki, W., Higgins, W., Janowiak, J., Mo, K.C., Ropelewski, C., Wang, J., Leetmaa, A., Reynolds, R., Jenne, R., Joseph, D.: The NCEP/NCAR 40-year reanalysis project, B. Am. Meteorol. Soc., 77 (3), 437-471, 1996.

Kirchhofer, W.: Climatological atlas of Switzerland. Meteoswiss, Federal Office of Topography swisstopo, 2000.

Knox, J.C.: Sensitivity of modern and Holocene floods to climate change, Quaternary Sci. Rev., 19 (1-5), 439-457, 2000.

Lehmann, C., Naef, F.: Die Größe der extremen Hochwasser der Lütschine, Tiefbauamt des Kanton Bern, Bern, 2003

Luterbacher, J., Xoplaki, E., Dietrich, D., Rickli, R., Jacobeit, J., Beck, C., Gyalistras, D., Schmutz, C., Wanner, H.: Reconstruction of sea level pressure fields over the Eastern North Atlantic and Europe back to 1500, Climate Dyn., 18 (7), 545-561, 2002.

Luterbacher, J., Dietrich, D., Xoplaki, E., Grosjean, M., Wanner, H.: European seasonal and annual temperature variability, trends, and extremes since 1500, Science 303 (5663), 1499-1503, 2004.

Magny, M., Bégeot, C., Guiot, J., Peyron, O.: Contrasting patterns of hydrological changes in Europe in response to Holocene climate cooling phases, Quaternary Sci. Rev., 22 (15-17), 1589-1596 , 2003.

Mudelsee, M., Börngen, M., Tetzlaff, G., Grünewald, U.: Extreme floods in central Europe over the past 500 years: Role of cyclone pathway “Zugstrasse Vb”, J. Geophys. Res. Atmos., 109 (D23), 2156-2202, 2004.

Müller, M., Kaspar, M.: Association between anomalies of moisture flux and extreme runoff events in the south-eastern Alps, Nat. Hazards Earth Sys., 11, 915-920, 2011.

Ortega, J.A., Garzón, G.: A contribution to improved flood magnitude estimation in base of palaeoflood record and climatic implications – Guadiana River (Iberian Peninsula), Nat. Hazard Earth Sys., 9, 229-239, 2009

Percival, D.B., Walden, A.T.: Spectral Analysis for physical Applications, Cambridge University Press, Cambridge, 1993.

Peristykh, A.N., Damon, P.E.: Persistence of the Gleissberg 88-year solar cycle over the last ~12,000 years: Evidence from cosmogenic isotopes, J. Geophys. Res., 108 (A1), 1003, doi:10.1029/2002ja009390, 2003.

Pfister, C.: Wetternachhersage: 500 Jahre Klimavariationen und Naturkatastrophen, Paul Haupt Verlag, Bern, 1999.

Pfister, C., Hächler S.: Überschwemmungskatastrophen im Schweizer Alpenraum seit dem Spätmittelalter. Raum-zeitliche Rekonstruktion von Schadenmustern auf der Basis historischer Queilen, Würzburger Geographische Arbeiten 80, 127-148, 1991.

Rogers, M.L., Richards, M.T., Richards, D. St. P.: Long-term variability in the length of the solar cycle, Astrophysics: arXiv: astro-ph/0606426v3, 15 p., 2006.

Röthlisberger, G.: Chronik der Unwetterschäden in der Schweiz, Berichte der Eidgenössischen Forschungsanstalt für Wald, Schnee und Landschaft 330, 122 pp , 1991.

Schmocker-Fackel, P., Naef, F.: More frequent flooding? Changes in flood frequency in Switzerland since 1850, J. Hydrol., 381 (1-2), 1-8, 2010a.

Schmocker-Fackel, P., Naef, F.: Change in flood frequencies in Switzerland since 1500, Hydrol. Earth Syst. Sc., 14, 1581-1594, 2010b.

Schulte, L., Julià, R., Oliva, M., Burjachs, F., Veit, H., Carvalho, F.: Sensitivity of Alpine fluvial environments in the Swiss Alps to climate forcing during the Late Holocene. Sediment Dynamics in Changing Environments, International Association of Hydrological Sciences Publications, 325, 367-374, 2008.

Schulte, L., Veit, H., Burjachs, F., Julià, R.: Lütschine fan delta response to climate variability and land use in the Bernese Alps during the last 2400 years, Geomorphology, 108 (1-2), 107-121 , 2009a.

Schulte, L., Julià, R., Veit, H., Carvalho, F.: Do high resolution fan delta records provide a useful tool for hazard assessment in mountain regions?, International Journal of Climate Change Strategies and Management, 1 (2), 197-210, 2009b.

Schulte, L., Carvalho, F., Peña, J.C., Baró, M., Julià, R., Burjachs F., Lomax J., Villanueva, I., Rubio, P., Veit, H.: Trying to understand mountain flood dynamics from multiproxy data: a 4600-year high resolution record from the Swiss Alps, Quatern. Int., 279-280, 2012.

Schulte, L., Peña, J.C., Julià, R., Carvalho, F., Llorca, J., Losada, J., Burjachs, F., Schmidt, T., Rubio, P., Veit, H.: Climate forcing of paleofloods in the Swiss Alps. In: Schnabel, S., Gómez Gutiérrez, A. (Eds.), Avances de la Geomorfología en España 2012-2014, XIII Reunión Nacional de Geomorfología, 143-146, 2014.

Schulz, M., Statteger, K.: SPECTRUM: Spectral analysis of unevenly spaced paleoclimatic time series, Comput. Geosci., 23 (9), 929-945, 1997.

Schulz, M., Mudelsee, M., REDFIT: Estimating red-noise spectra directly from unevenly spaced paleoclimatic time series, Comput. Geosci., 28 (3), 421-426, 2002.

Shackleton, N.J.: The 100,000-year ice-age cycle identified and found to lag temperature, carbon dioxide, and orbital eccentricity, Science, 289 (5486), 1897-1902, 2000.

Siegel, A.F., 1979. The noncentral chi-squared distribution with zero degrees of freedom and testing for uniformity, Biometrika 66 (2), 381-386.

Solanki, S.K., Fligge, M.: Reconstruction of past solar irradiance, Space Sci. Rev., 94 (1-2), 127-138, 2000.

Stuiver, M., Braziunas, T.F., Grootes, P.M., Zielinski, G.A.: Is there evidence for solar forcing of climate in the GISP2 Oxygen Isotope record?, Quaternary Res., 48 (3), 259-266, 1997.

Stuiver, M., Grootes, P.M.: GISP2 Oxygen Isotope Ratios, Quaternary Res., 53 (3), 277-284, 2000.

Tinner, W., Lotterb, A.F., Ammann, B., Conederac, M., Hubschmida, P., van Leeuwena, J.F.N., Wehrlia, M.: Climatic change and contemporaneous land-use phases north and south of the Alps 2300 BC to 800 AD, Quaternary Sci. Rev., 22 (14), 1447-1460, 2003.

van Bebber, W. J.: Die Zugstrassen der barometrischen Minima nach den Bahnenkarten der Deutschen Seewarte für denZeitraum von 1870–1890, Meteorol. Z., 8, 361–366, 1891.

Vaquero, J.M.: Solar signal in the number of floods recorded for the Tagus river basin over the last millennium, Climatic Change, 66 (1-2), 23-26, 2004.

Versteegh, G.J.M.: Solar Forcing of Climate. 2: Evidence from the Past, Space Sci. Rev., 120 (3-4), 243-286, 2005.

Vischer, D.: Die Geschichte des Hochwasserschutzes in Schweiz: von den Anfängen bis ins 19. Jahrhundert, Bundesamt für Wasser und Geologie, Bern, 2003.

Vonmoos, M., Beer, J., Muscheler, R.: Large variations in Holocene solar activity: Constraints from ^{10}Be in the Greenland Ice Core Project ice core, J. Geophys. Res.: Space Physics 111 (A10), A10105. DOI: 10.1029/2005JA011500, 2006.

Weingartner, R., Reist, T.: Gotthelfs „Wassernot im Emmental“ – Hydrologische Simulation des Extremhochwassers vom 13. August 1837. In: Pfister, Ch., Summermatter, S. (Eds.), Katastrophen und ihre Bewältigung – Perspektiven und Positionen, Berner Universitätsschriften, Band 49, Haupt-Verlag, 21-41, 2004.

Wetter, O., Pfister, Ch., Weingartner, R., Luterbacher, J., Reist, T., Trösch, J.: The largest floods in the High Rhine basin since 1268 assessed from documentary and instrumental evidence, Hydrol. Sci. J., 56 (5), 733-758, 2011.

Wilhelm, B., Arnaud, F., Sabatier, P., Crouzet, Ch., Brisset, E., Chaumillion, E., Disnar, J.R., Guiter, F., Malet, E., Reyss, J.L., Tachikawa, K., Bard, E., Delannoy, J.J.: 1400 years of extreme precipitation patterns over the Mediterranean French Alps and possible forcing mechanisms, Quaternary Res., 78 (1), 1–12, 2012.

Wirth, S., Gilli, A., Simonneau, A., Ariztegui, D., Vannière, B., Glur, L., Chapron, E., Magny, M., Anselmetti, F.: A 2000 year long seasonal record of floods in the southern European Alps, Geophysical Research Letters 40, 4025-4029, doi: 10.1002/2009grl.50741, 2013a.

Wirth, S., Glur, L., Gilli, A., Anselmetti, F.: Holocene flood frequency across the Central Alps – solar forcing and evidence for variations in North Atlantic atmospheric circulation, Quaternary Sci. Rev., 80, 112-128, 2013b.

Links to the different data are as follows:

1) The annual average sunspot for the period between 1700 and 2011, data available online through the website: http://www.sidc.be/sunspot-data/

2) Annually resolved ^{10}Be data (Berggren et al., 2009) are available from Greenland in: ftp://ftp.ncdc.noaa.gov/pub/data/paleo/icecore/greenland/summit/ngrip/ngrip-10be.txt

3) Volcanic Eruptions for the Northern Hemisphere for the period 1800-2000 are available in: http://climate.envsci.rutgers.edu/IVI2/

4) Annually resolved δ^{18}O data (Stuiver and Grootes, 2000) are available in: http://depts.washington.edu/qil/datasets/gisp2_main.html

5) Twentieth Century Reanalysis Project (Compo et al., 2011) dataset available in: http://www.esrl.noaa.gov/psd/data/gridded/data.20thC_ReanV2.html

6) Reconstruction of Sea Level Pressure fields over the eastern North Atlantic and Europe back to 1500 (Luterbacher et al., 2002) dataset available online in: http://www.ncdc.noaa.gov/paleo/pubs/luterbacher2002/luterbacher2002.html

7) The Annual Temperature of Switzerland (ALP-IMP, 2006) available online in: http://www.zamg.ac.at/ALP-IMP/

Table 1. Principal statistical parameters of SNAO for each of the categories of the flood damage index INU whose thresholds were defined according to the standard deviation (SD).

	INU_i > 0 SD	**INU_i > 1.0 SD**	**INU_i > 2.5 SD**	**INU_i > 5.0 SD**
Average	**0.04**	**0.10**	**0.18**	**0.45**
SNAO + (years)	20	11	6	4
SNAO – (years)	13	7	3	0
N	33	18	9	4
Max	1.41	0.94	0.84	0.81
Min	-1.93	-1.12	-0.79	0.10
P95	1.18	0.90	0.83	0.77
P2	-1.76	-1.08	-0.74	0.12

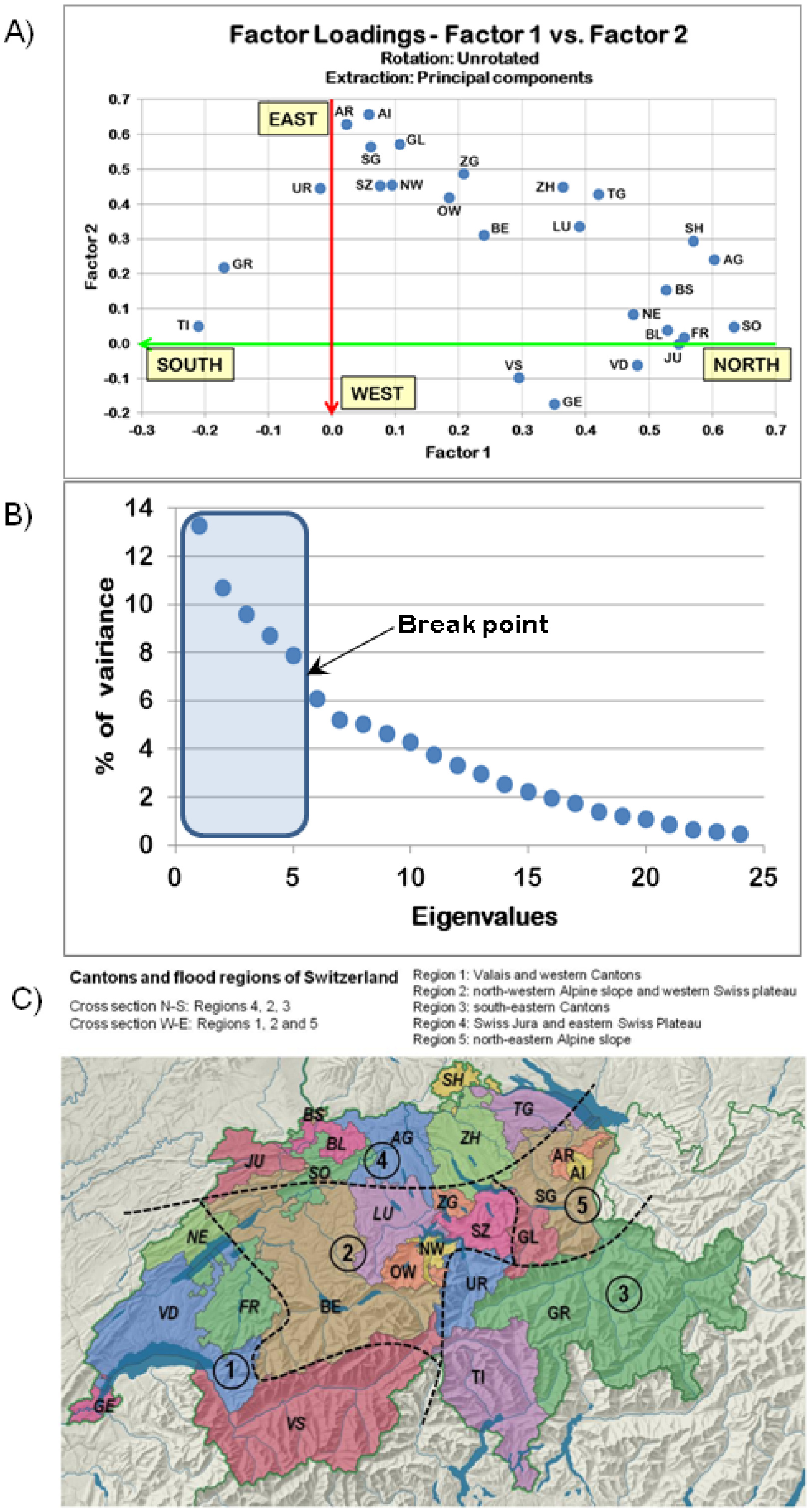

Fig. 1: A) Factor loadings of Factor 1 versus Factor 2 after the application of the PCA to the flood matrix without rotation. B) Scree-test and number of components selected. C) Regionalization of Switzerland according to the PCA applying the Equamax Rotation. Dotted lines are the limits of the regions (DEM from Atlas of Switzerland, 2004; map modified).

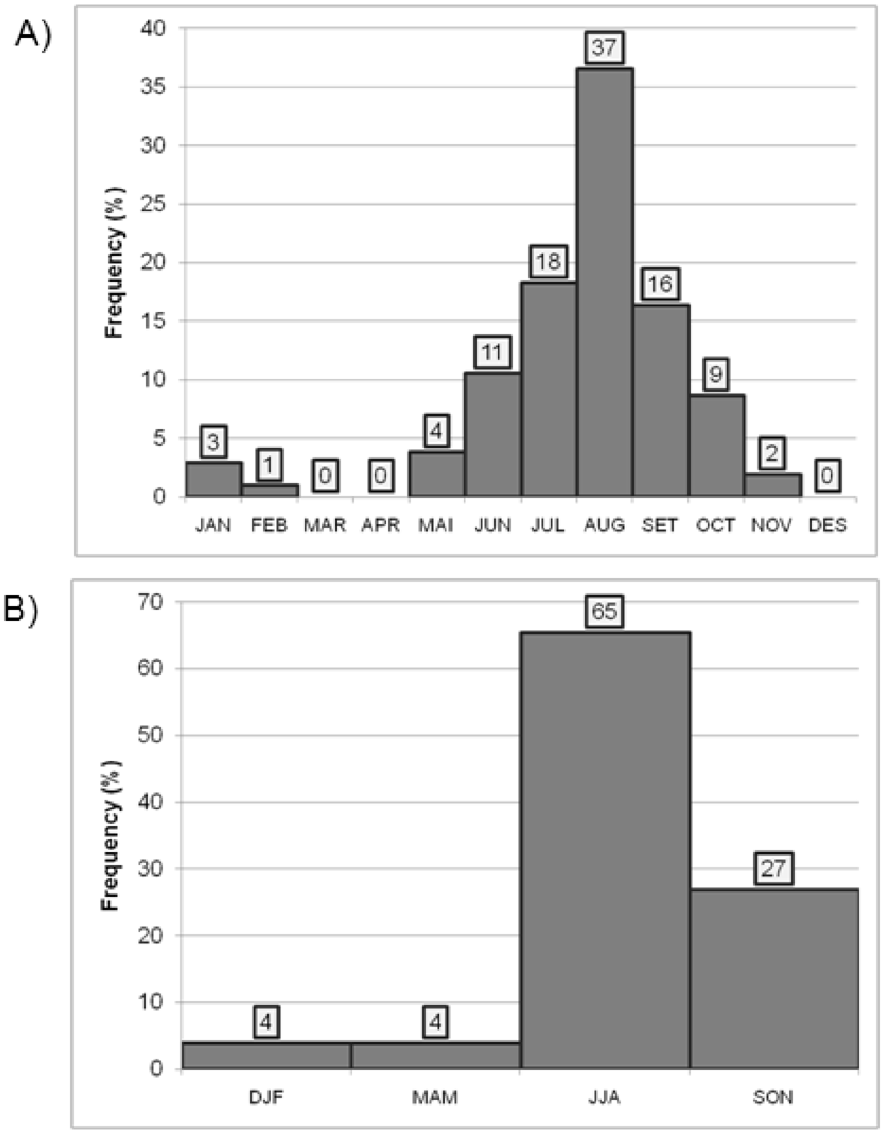

Fig. 2: A) Monthly distribution of major floods in Switzerland for the period 1800-2009 for very severe (VS) and catastrophic (C) flood categories. B) Seasonal distribution of VS and C floods. DJF: December-January-February; MAM: March-April-May; JJA: June-July-August; SON: September-October-November.

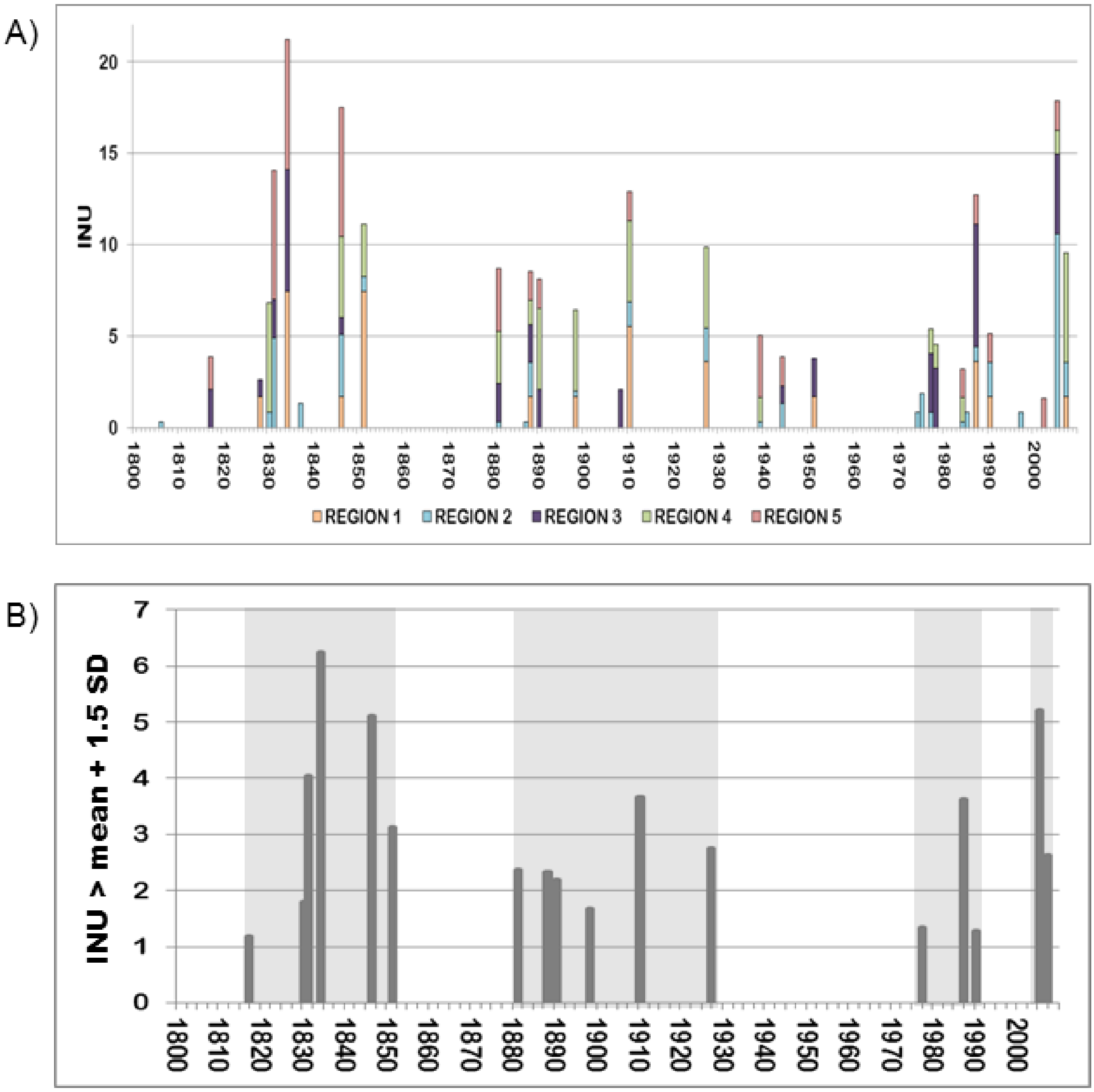

Fig. 3: A) Regional flood damage index INU for the period 1800-2009. B) Values of INU that exceed 1.5 times the standard deviation. The periods with a high frequency of flooding are shaded grey.

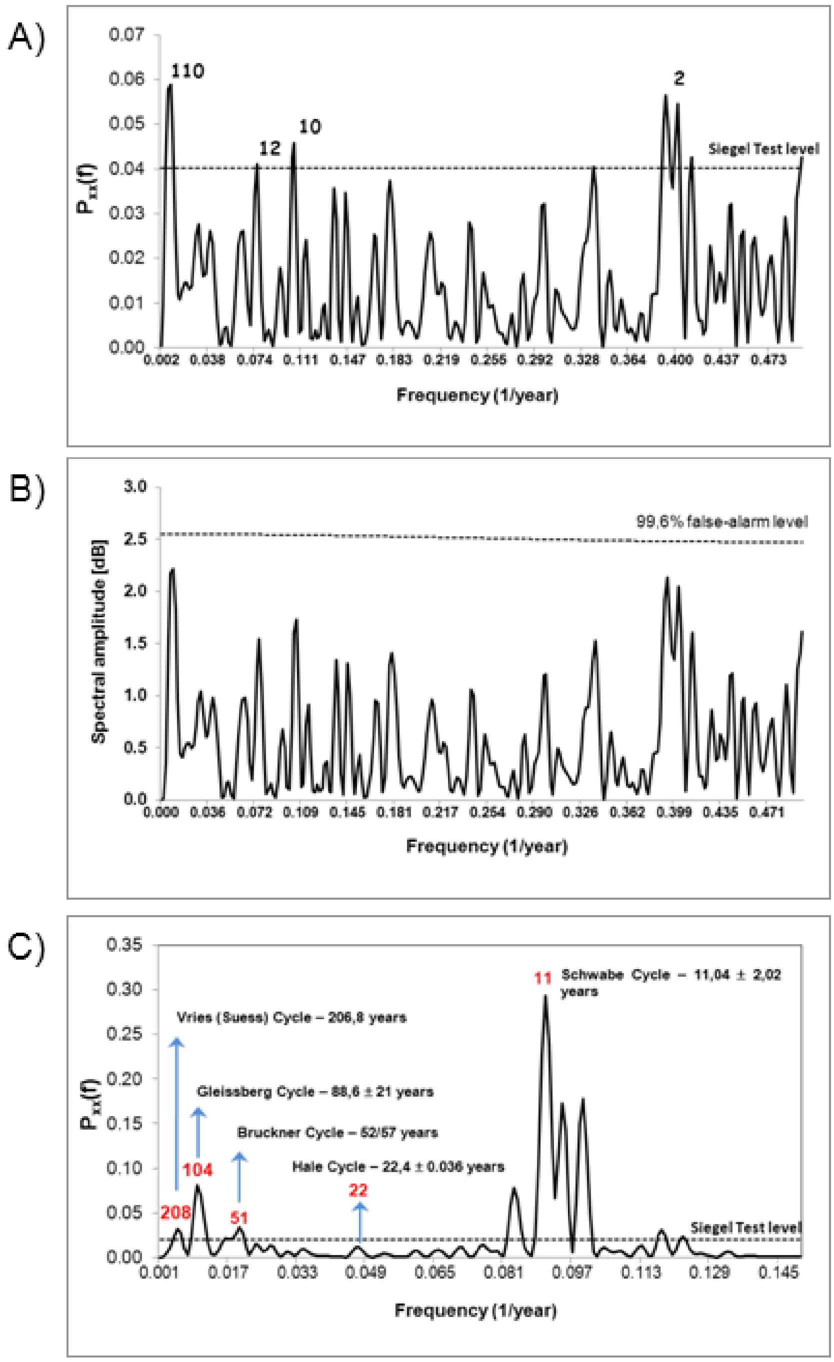

Fig. 4: A) Harmonic analysis for the summer flood damage index INU. Dotted line represents critical level for the Siegel test and significant frequencies are shown in years. B) Red noise AR1 spectra of INU. Dotted line shows false-alarm level. C) Harmonic analysis for the average annual number of sunspots. Dotted horizontal lines represent critical levels for the Siegel test. Significant frequencies are shown in years. The principal solar cycles are highlighted.

A)

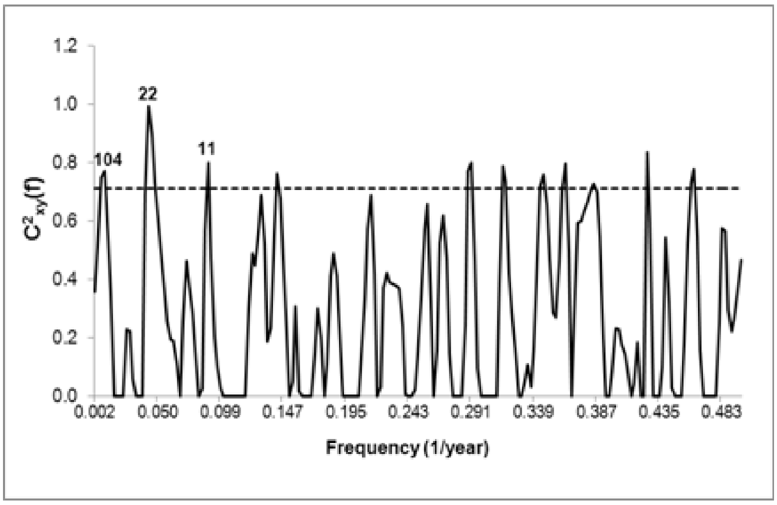

B)

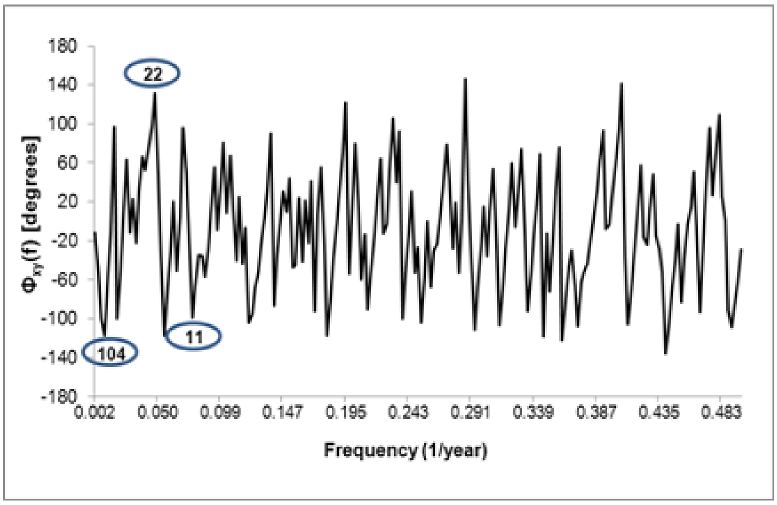

Fig. 5: Cross-spectral analysis between the index of summer flood damage INU and annual number of sunspots: A) Coherency spectrum. Dashed line indicates false-alarm level for α = 0.1. B) Phase spectrum. The sign of the INU data was changed prior to cross-spectral analysis in order to prevent an artificial phase offset by ±180º. Negative angles indicate that the maximum frequency in the floods occurs during a solar activity minimum and vice versa.

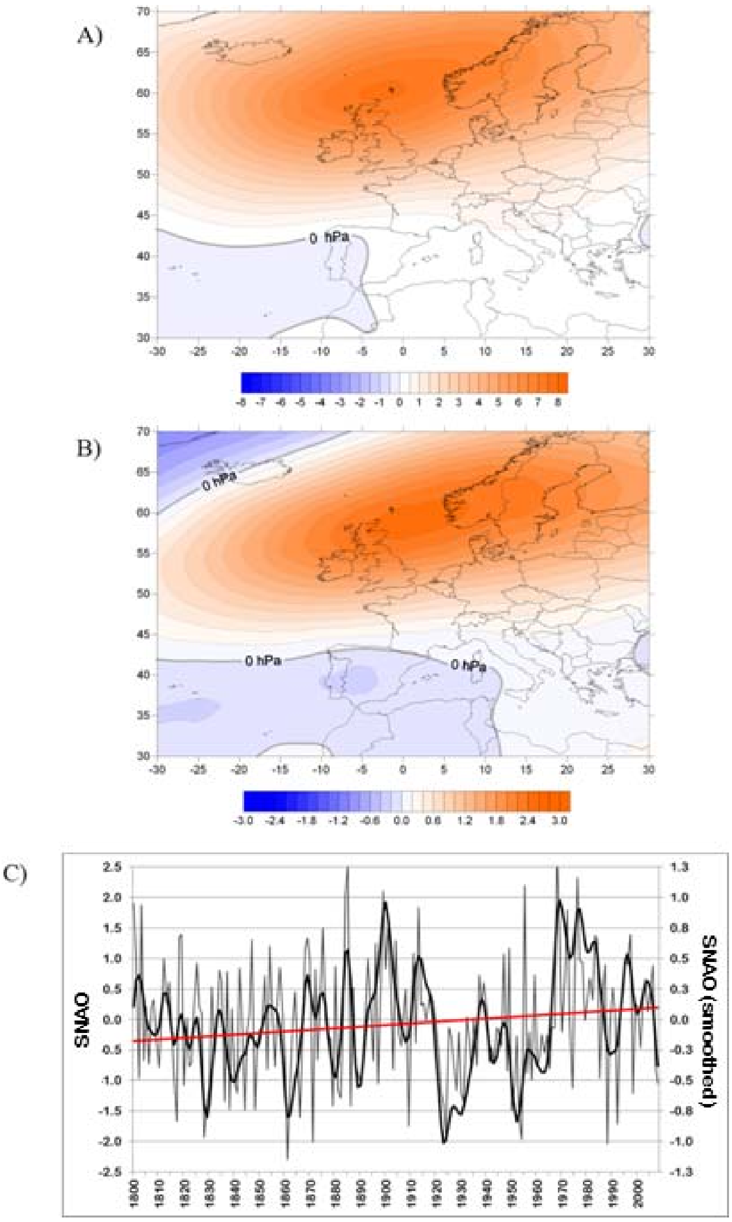

Fig. 6: A) Principal mode of low-frequency atmospheric circulation based on principal eigenvector extracted from PCA in S-mode, using the covariance matrix of monthly EMSLP for the period 1871-2009 (Summer North Atlantic Oscillation, SNAO). This has been applied to the grid extracted of the 20th Century Reanalysis project (Compo et al., 2011). Red (blue) contours show positive (negative) anomalies. B) As in A) but applied to the monthly EMSLP of the Luterbacher Reanalysis Grid (Luterbacher et al., 2002) for the period 1800-1999. C) Time series of the SNAO pattern for the period 1800-2009 (thin black line) smoothed by a low-pass Gaussian filter of 11 years (black line). Red line is the trend of the SNAO time series (significant and positive trend at a 95% confidence level, p-value= 0.006).

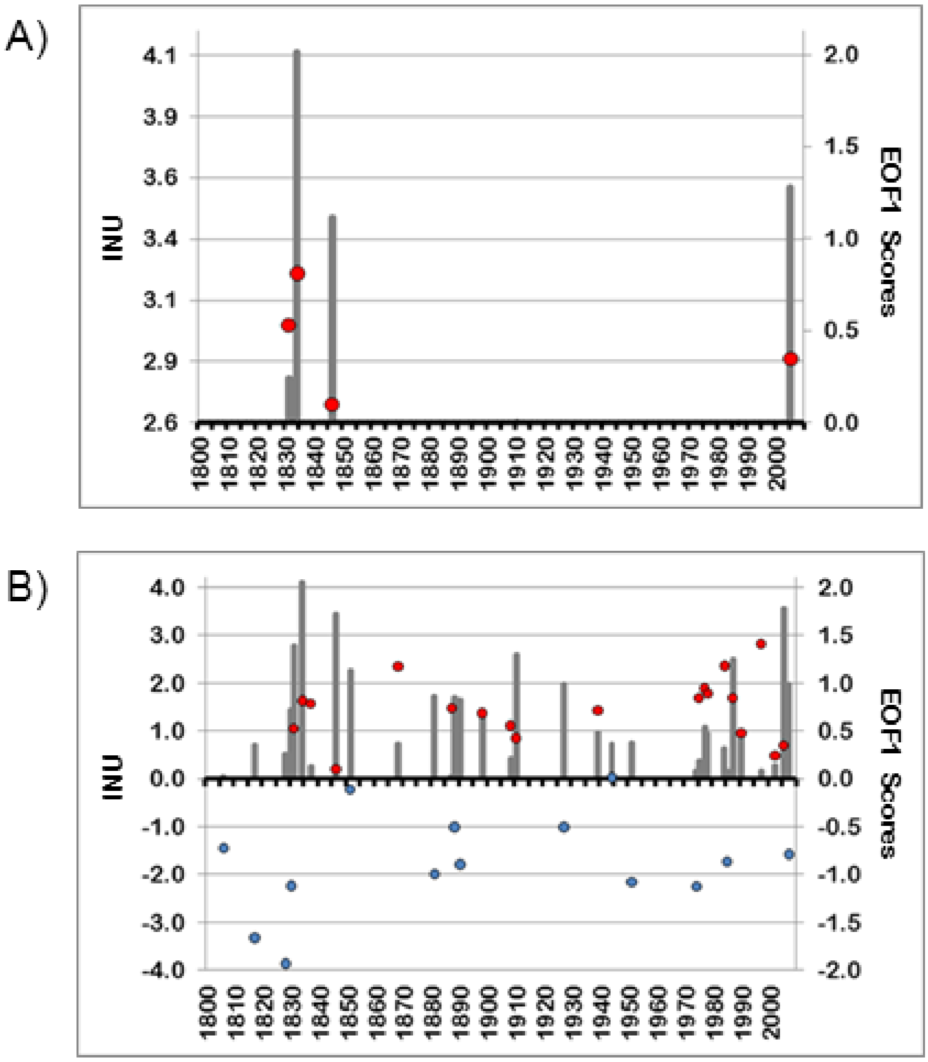

Fig. 7: A) Summer flood damage index INU (bars) versus positive phase of SNAO (red dots) for values of INU five times greater than the standard deviation (INU >5 SD). B) As in A) but for the complete signal of the INU. Blue dots represents negative SNAO phase.

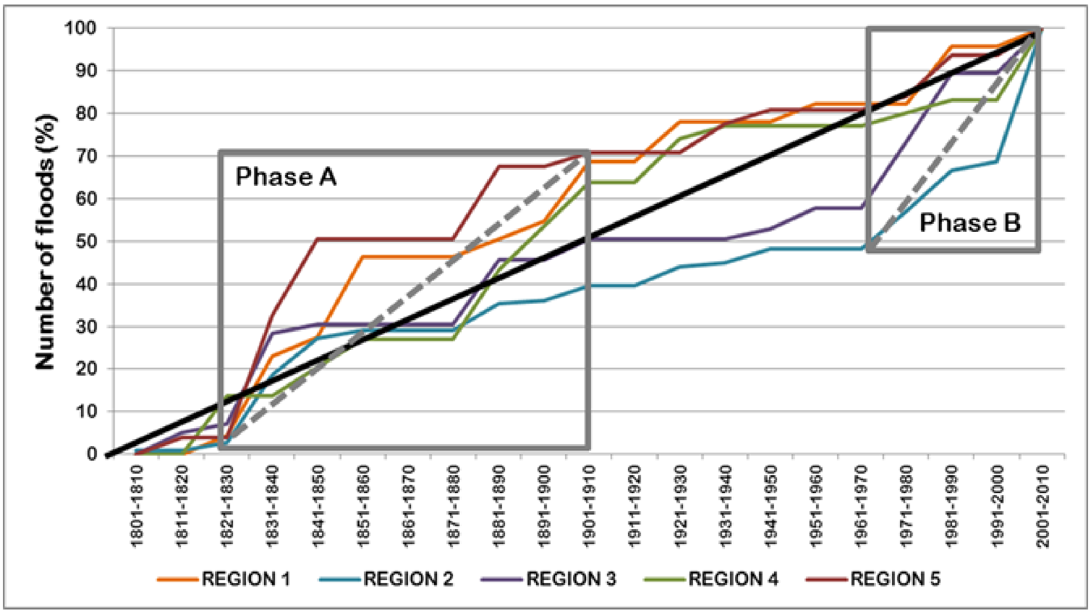

Fig. 8: Cumulative number of floods (in %) versus time, for each region: the cumulative frequencies are obtained by adding the absolute frequencies of all years up to the year referred to. Black line: Bisector of the quadrant where the distribution of the floods is perfect.

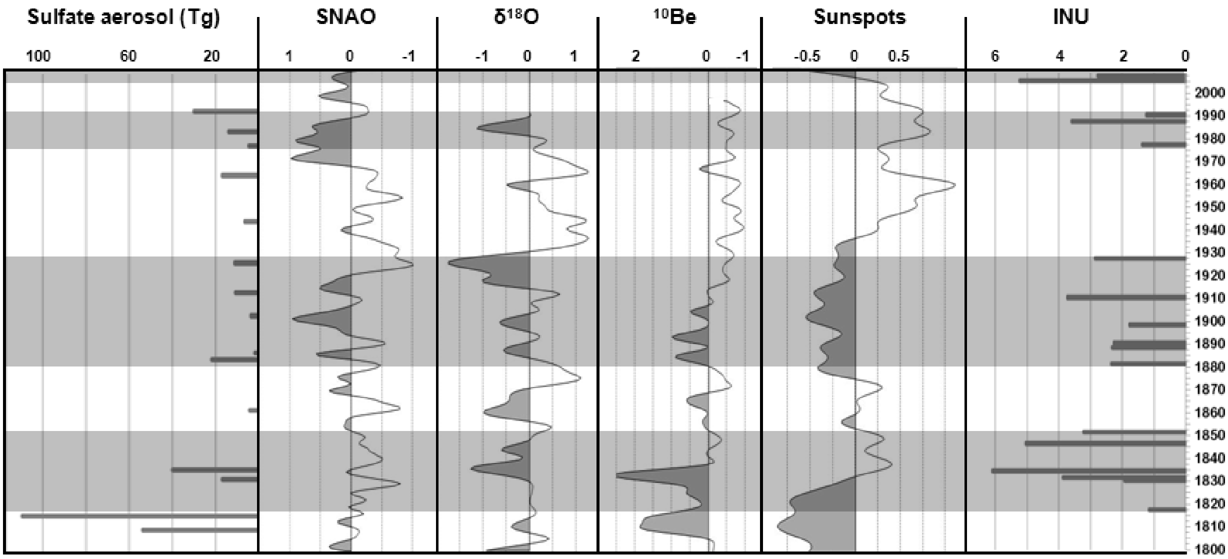

Fig. 9: Temporal evolution of INU (INU >1.5 SD), the volcanic eruptions and the standardized anomalies of SNAO, $\delta^{18}O$, ^{10}Be, sunspots for the period 1800-2009. All series are plotted as normalized values smoothed with an 11-year low-pass Gaussian filter, except the sunspot number record smoothed with a 22-year filter. The volcanic eruptions and INU index are unsmoothed. Periods of high flood frequency are marked on the chart. Note that the $\delta^{18}O$ and sunspot scales are reversed.

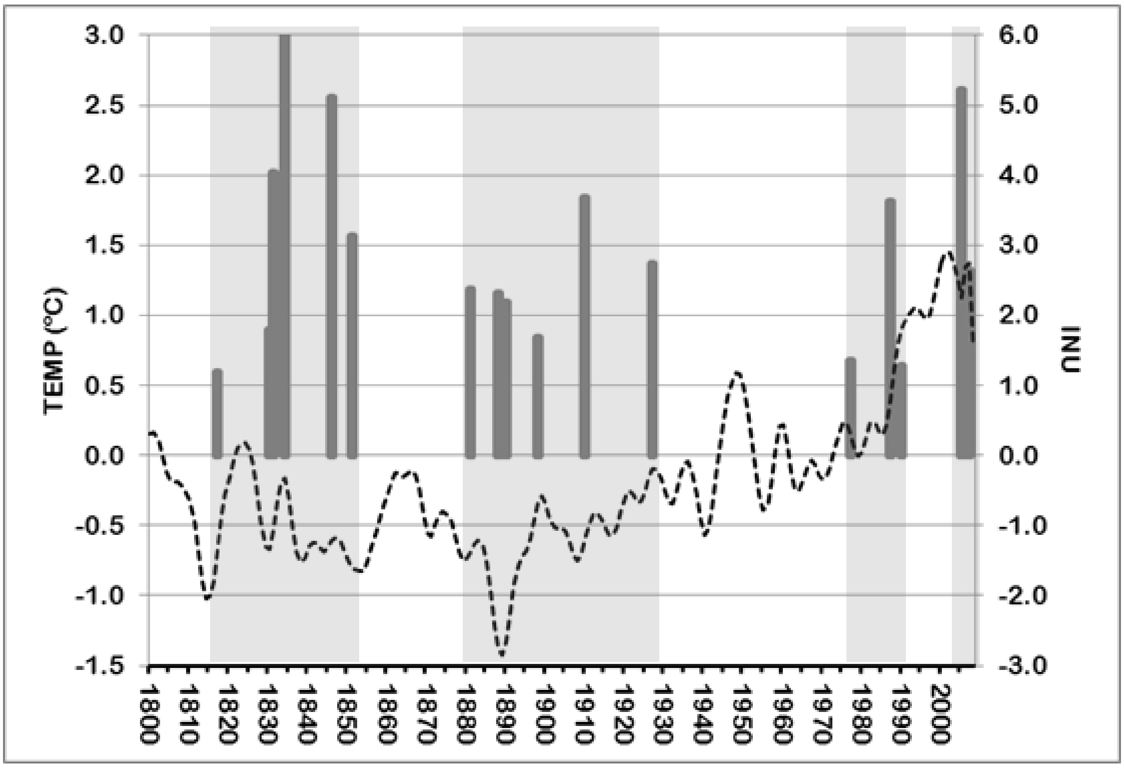

Fig. 10: Temporal evolution of the standardized anomalies of INU (full line; INU >1.5 SD) and the annual average temperature for Switzerland (dashed line) for the period 1800-2009. Both series are plotted as normalized values and temperature data is smoothed with an 11-year low-pass Gaussian filter.

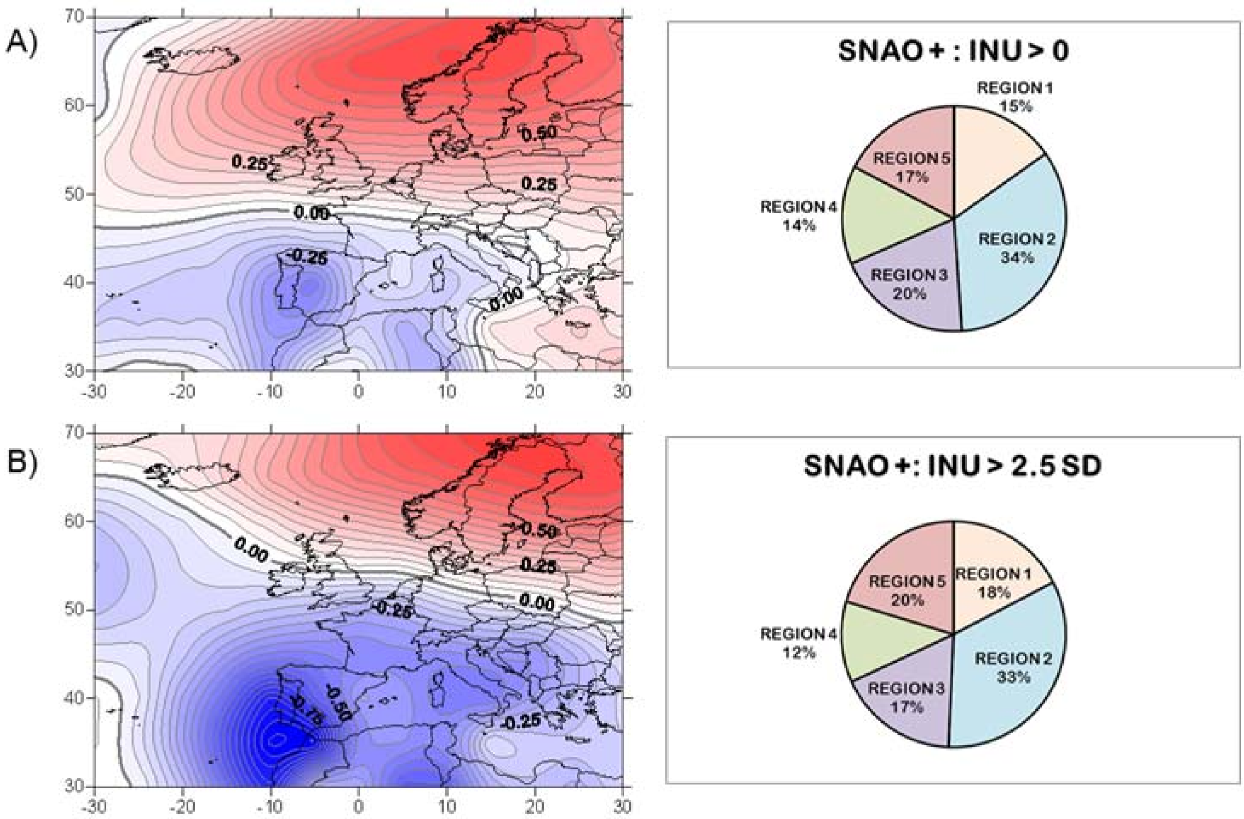

Fig. 11: A) Left: Composites of monthly EMSLP extracted of 20CRP plus the Luterbacher Reanalysis grids of the years with SNAO in positive phase and INU>0. The units are expressed in hPa. Red (blue) contours show positive (negative) anomalies. Right: number of floods in percentage by region. B) is as A) but for the years with INU >2.5 SD. Region 1: Valais and the western cantons; region 2: western part of the northern slope of the Alps and Swiss plateau; region 3: Grisons plus the southern flank of the Alps; region 4: eastern Jura and Swiss Plateau; region 5: eastern part of the northern flank of the Alps.

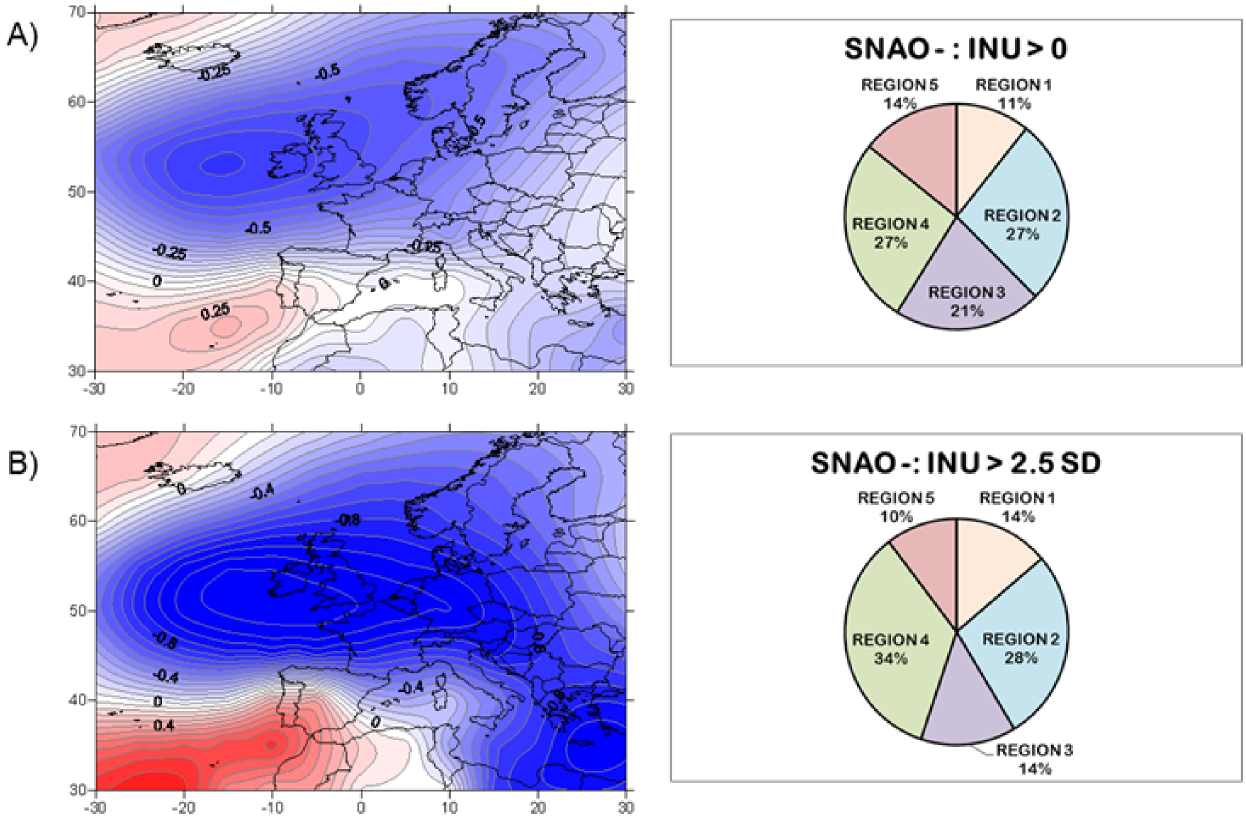

Fig. 12: As in Fig.11 but for SNAO negative phase. Region 1: Valais and the western cantons; region 2: western part of the northern slope of the Alps and Swiss plateau; region 3: Grisons plus the southern flank of the Alps; region 4: eastern Jura and Swiss Plateau; region 5: eastern part of the northern flank of the Alps.